ARTICLE

Impact of age and vector construct on striatal and nigral transgene expression

Nicole K Polinski[1,2], Fredric P Manfredsson[1,3], Matthew J Benskey[1], D Luke Fischer[1], Christopher J Kemp[1], Kathy Steece-Collier[1,3], Ivette M Sandoval[1], Katrina L Paumier[1] and Caryl E Sortwell[1,3]

Therapeutic protein delivery using viral vectors has shown promise in preclinical models of Parkinson's disease (PD) but clinical trial success remains elusive. This may partially be due to a failure to include advanced age as a covariate despite aging being the primary risk factor for PD. We investigated transgene expression following intracerebral injections of recombinant adeno-associated virus pseudotypes 2/2 (rAAV2/2), 2/5 (rAAV2/5), 2/9 (rAAV2/9), and lentivirus (LV) expressing green fluorescent protein (GFP) in aged versus young adult rats. Both rAAV2/2 and rAAV2/5 yielded lower GFP expression following injection to either the aged substantia nigra or striatum. rAAV2/9-mediated GFP expression was deficient in the aged striatonigral system but displayed identical transgene expression between ages in the nigrostriatal system. Young and aged rats displayed equivalent GFP levels following LV injection to the striatonigral system but LV-delivered GFP was deficient in delivering GFP to the aged nigrostriatal system. Notably, age-related transgene expression deficiencies revealed by protein quantitation were poorly predicted by GFP-immunoreactive cell counts. Further, *in situ* hybridization for the viral CβA promoter revealed surprisingly limited tropism for astrocytes compared to neurons. Our results demonstrate that aging is a critical covariate to consider when designing gene therapy approaches for PD.

Molecular Therapy — Methods & Clinical Development (2016) **3**, 16082; doi:10.1038/mtm.2016.82; published online 7 December 2016

INTRODUCTION

Viral vectors are useful tools to deliver genes to the central nervous system (CNS), allowing stable expression of an exogenous protein, short hairpin RNA, or other genomic material. The benefits of viral vectors include site-specific expression, delivery of transgenes to dividing and nondividing cells, stable transgene expression, and targeted tropism.[1,2] These benefits, along with an improved safety profile, have led to the use of viral vector-mediated gene therapy to treat diseases of the difficult-to-target CNS or to generate animal models of CNS disorders.[1–8] In particular, gene therapy is currently being explored in clinical trials for Alzheimer's disease (AD)[1,4] and Parkinson's disease (PD)[1,3]—two diseases in which there are no disease-modifying treatments and symptomatic treatments only provide a moderate benefit.[9–11] Multiple clinical trials have completed phase 1 safety testing for viral vector-mediated gene therapy in PD.[1,3] Unfortunately, the early phase 2 efficacy trials have not shown improvement beyond the placebo effect or above levels currently achieved with symptomatic treatments.[1] While limitations in the predictive validity of PD models likely impact translation of gene therapy to the clinic, consideration should also be given to the fact that preclinical studies almost exclusively use young adult animals.[12–18] Age is the single greatest risk factor for developing PD and previous results demonstrate that age can dramatically influence therapeutic efficacy in PD models.[19,20] In the case of trophic factor gene therapy for PD, it is likely that transgene expression must reach a critical threshold in order to be therapeutically effective. Understanding the impact of age on viral vector transduction efficiency is required for the design of successful gene therapy for PD.

The two most common vector classes used for delivery of genes to the CNS are recombinant adeno-associated virus (rAAV) and lentivirus (LV).[1,5–7,21] The transduction properties of these recombinant vector classes have been extensively characterized in the CNS of young adult animals, with both resulting in stable transduction that can last years after injection.[1,2,22–24] Limited evidence suggests that the age of the transduced subject can negatively impact the efficiency of certain rAAV pseudotypes. For example, aged rat septal neurons have been shown to be relatively resistant to transduction mediated by rAAV2/2.[25] Further, we have documented a robust deficiency in rAAV2/5-mediated transduction of the substantia nigra pars compacta (SNpc) in aged as compared to young adult rats.[7,26] Taken together, this limited evidence suggests certain vectors may not perform as efficiently in the aged brain.

To directly address this concern, the present study compared the ability of three rAAV and one LV vector to deliver transgene to the young adult (3 months) and aged (20 months) rat brain. The constructs chosen were rAAV2/2, rAAV2/5, rAAV2/9, and LV pseudotyped with vesicular stomatitis virus (VSV-G) due to previous reports of transduction changes[25,26]—or lack thereof[27]—with

[1]Department of Translational Science and Molecular Medicine, Michigan State University, Grand Rapids, Michigan, USA; [2]Neuroscience Graduate Program, Michigan State University, East Lansing, Michigan, USA; [3]Mercy Health Saint Mary's, Grand Rapids, Michigan, USA. Correspondence: CE Sortwell (caryl.sortwell@hc.msu.edu)

age and relevance to PD preclinical and clinical trials.[1,3,12–17,25–27] The respective viral vectors, expressing a green fluorescent protein (GFP) transgene, were unilaterally injected into either the SNpc to transduce the nigrostriatal system or into the striatum to transduce the striatonigral system. The striatum is the structure most often targeted in PD gene therapy clinical trials.[3,13,16,28] Transgene expression was assessed by quantifying GFP immunoreactive cells, GFP protein levels in anterograde structures, as well as GFP mRNA expression via qPCR and *in situ* hybridization. Since the ultimate goal of trophic factor gene therapy is protein delivery, we designated Western blot measures of GFP protein expression in anterograde structures as the primary outcome measure. Using this criterion, our results show a significant decrease in transgene expression in the aged *nigrostriatal* system using rAAV2/2, rAAV2/5, and LV, but not rAAV2/9. In contrast, in the aged *striatonigral* system, rAAV2/2, rAAV2/5, and rAAV2/9 express lower transgene levels with age whereas LV is equally as efficient between ages. Our results demonstrate that advanced age impacts the efficacy of viral vectors, with most—but not all—viral vectors impaired in the aged versus young adult rat brain.

RESULTS

Previous reports have found transduction deficiencies in the aged rat following injection of rAAV2/2 in the septum, rAAV2/5 in the SN, but not with rAAV2/9 in the SN.[25–27] However, systematic comparison of the impact of age and brain region on viral vector transduction efficiency is lacking. In order to validate and expand previous findings, we sought to investigate the generalizability of this age-related deficiency to various vector constructs and an additional brain structure by systematically characterizing the changes in transduction efficiency with age. To accomplish this, we injected rAAV2/2, rAAV2/5, rAAV2/9, or LV expressing GFP driven by the chicken beta actin/cytomegalovirus enhancer (CβA/CMV) promoter hybrid into the SNpc to target the nigrostriatal system, or into the striatum to target the striatonigral system (Supplementary Figure S1). At 1 month postinjection, when transgene expression levels asymptote,[22] we assessed transduction efficiency at the injection site with immunohistochemical or RNA measures, as well as transgene expression in the anterograde structure (striatum following SNpc injection, or SN pars reticulata (SNpr) following striatal injection) using Western blotting for GFP to measure system-specific transduction. To preclude signal resulting from retrograde transport of the viral vectors, special care was taken with SNpr samples to avoid inclusion of SNpc tissue in the microdissection (Supplementary Figure S2). In addition, to ensure any changes in GFP expression with age were not due to age-related neuronal loss or vector-related toxicity, we quantified the number of tyrosine hydroxylase immunoreactive (TH+) neurons in the SNpc of young adult and aged rats. No significant difference was found for either age or vector injection for rAAV2/2 GFP (age: $F_{(1,5)} = 2.90$, $P = 0.149$; injection: $F_{(1,5)} = 0.421$, $P = 0.545$; Supplementary Figure S3a), rAAV2/9 GFP (age: $F_{(1,12)} = 0.029$, $P = 0.868$; injection: $F_{(1,12)} = 1.98$, $P = 0.185$; Supplementary Figure S3b), rAAV2/5 GFP (age: $F_{(1,11)} = 4.63$, $P = 0.054$; injection: $F_{(1,11)} = 0.63$, $P = 0.444$; Supplmentary Figure S3c), or LV GFP (age: $F_{(1,7)} = 0.05$, $P = 0.833$; injection: $F_{(1,7)} = 0.81$, $P = 0.398$; Supplementary Figure S3d), as has been reported previously.[26,29]

Experiment 1. Vector transgene expression levels in the nigrostriatal system and midbrain following intranigral injections to the young adult and aged rat
Age-related decreases in exogenous GFP protein in the nigrostriatal system are observed with rAAV2/2, rAAV2/5, and LV, but not rAAV2/9

intranigral injections. To investigate transgene expression in the nigrostriatal system, we quantified GFP protein in the anterograde striatal structure at one month postinjection into the SNpc. This approach allowed us to avoid inclusion of GFP protein within nondopaminergic neurons in the SN and ventral mesencephalon that also are transduced following SNpc vector injections.[26,30,31] GFP protein level was our primary outcome measure to assess transgene delivery due to the fact that adequate protein expression is the primary determinant of functional and neuroanatomical benefits of viral vector-mediated gene therapy.[12] Aged rats displayed significantly lower levels of GFP in the striatum as compared to young adult rats following injection with three of the four vector constructs (Figure 1). Aged rat striatal tissue contained 62% less GFP following rAAV2/2 GFP transduction ($P = 0.005$; Figure 1a), 75% less GFP following rAAV2/5 GFP transduction ($P = 0.043$; Figure 1c), and 57% less GFP following LV GFP transduction ($P = 0.016$; Figure 1d) as compared to their young adult rat counterparts. The sole viral vector that did not display decreased levels of transgene expression in the aged rat was rAAV2/9, which conversely, trended toward an increase in striatal GFP levels in the aged compared to young adult rat ($P = 0.087$; Figure 1b). These results demonstrate that advanced age presents a barrier to efficient transduction with many, but not all, of the viral vector constructs tested in the rat nigrostriatal system.

Age-related decreases in exogenous protein expression in the nigrostriatal system are not reflected by differences in total GFP-positive cells within the mesencephalon. To assess the relationship between the number of transduced cells in the mesencephalon and transduction efficiency in the nigrostriatal system, we first quantified the total number of GFP-positive (GFP+) cells throughout the midbrain with unbiased stereology. No significant differences were observed in total numbers of GFP+ cells in the midbrain following rAAV2/2 GFP ($P = 0.135$; Figure 2a), rAAV2/5 GFP ($P = 0.141$; Figure 2g), and LV GFP ($P = 0.307$; Figure 2j) injection into the aged as compared to young adult rat SNpc. However, following rAAV2/9 GFP injection into the SNpc, aged rats exhibited greater numbers of GFP+ cells in the midbrain as compared to young adult rats ($P = 0.037$; Figure 2d). To determine whether aging impacted the phenotype of cells expressing GFP, we quantified the ratio of GFP+ neurons to GFP+ glia (microglia and astrocytes). No differences were seen between ages in the percent of neurons, astrocytes, or microglia expressing GFP for any vector construct (Supplementary Figure S4a). The overwhelming majority (>98% for rAAV pseudotypes and >85% for LV) of GFP+ cells were neuronal following injection in the SNpc (Supplementary Figure S4; Supplementary Table S1). These results demonstrate that age-related decreases in transgene protein expression in the nigrostriatal system (Figure 1) are not readily detectable using total counts of GFP+ cells in the mesencephalon.

Quantification of GFP+/TH+ SNpc neurons reveals fewer GFP+ nigrostriatal dopamine neurons in aged rats injected with rAAV2/2 GFP and LV GFP. To investigate the number of transduced SNpc neurons specifically, we performed dual immunofluorescent labeling for GFP and TH (Figure 2b,e,h,k). rAAV2/2 GFP and LV GFP displayed a 47% ($P = 0.022$) and 35% ($P = 0.025$) reduction, respectively, in the number of nigrostriatal SNpc dopaminergic neurons expressing GFP in the aged brain as compared to the young adult rat brain (Figure 2b–c and Figure 2k–l). No significant differences in the number of SNpc dopaminergic neurons expressing GFP were observed between ages following rAAV2/5 GFP (p=0.356; Figure 2h–i) or rAAV2/9 GFP ($P = 0.184$; Figure 2e–f). The fact that decreases in striatal GFP levels in aged rats following intranigral injections (Figure 1) are associated
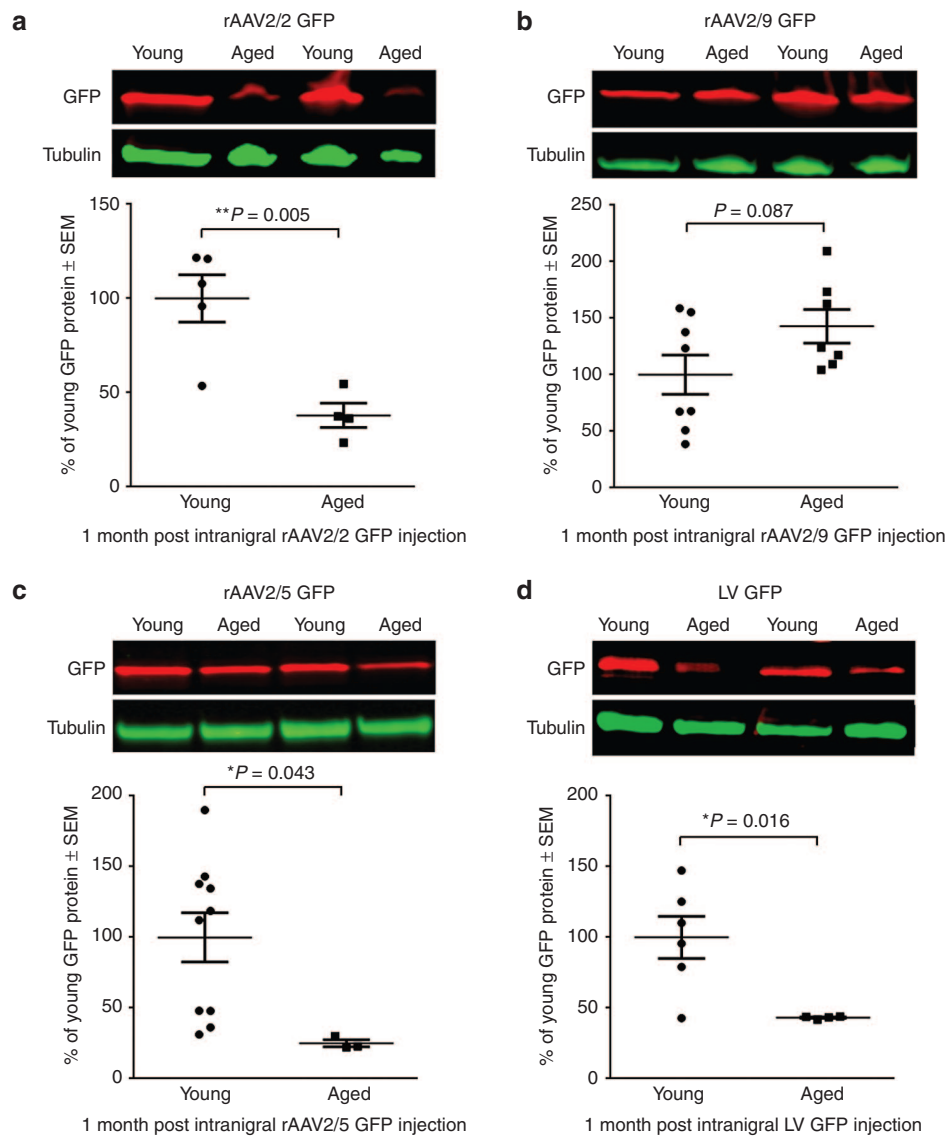
Figure 1 Viral vector-mediated expression of GFP is reduced in the aged nigrostriatal system with rAAV2/2, rAAV2/5, and LV, but not rAAV2/9. Representative Western blot and quantitation of GFP in striatal samples of young adult (Young) and aged (Aged) rats one month post-injection with (**a**) rAAV2/2 GFP, (**b**) rAAV2/9 GFP, (**c**) rAAV2/5 GFP, or (**d**) LV GFP. (**a**) Aged (n = 4) rats expressed significantly less striatal GFP than young adult (n = 5) rats following rAAV2/2 GFP transduction (**$P \leq 0.01$). (**b**) Young adult (n = 8) and aged (n = 7) rats expressed equivalent levels of GFP following rAAV2/9 GFP transduction (P > 0.05). (**c**) Aged (n = 3) rats expressed significantly less GFP than young adult (n = 10) rats following rAAV2/5 GFP transduction (*$P \leq 0.05$). (**d**) Aged (n = 4) rats expressed significantly less striatal GFP than young adult (n = 6) rats following LV GFP transduction (*$P \leq 0.05$). Values are expressed as the percent of the young mean optical density scores, with GFP signal normalized to tubulin controls ± SEM for each group. GFP, green fluorescent protein; LV, lentivirus; rAAV, recombinant adeno-associated virus; SEM, standard error of the mean.

with decreased GFP+/TH+ SNpc neurons in some (rAAV2/2, LV) but not all (rAAV2/5) vector constructs suggests that the dual labeling GFP/TH approach can be somewhat predictive of the impact of aging on vector-mediated transgene expression in the nigrostriatal system.

Age-related decreases in GFP mRNA are observed following intranigral injection with rAAV2/2, rAAV2/5, and LV, but not with rAAV2/9. To investigate whether age-related changes in GFP protein expression are due to deficiencies in steps of transduction upstream of protein synthesis, we used the complimentary approaches of qPCR and RNAscope *in situ* hybridization. qPCR was not conducted on the rAAV2/5 and LV SNpc due to lack of tissue availability. qPCR analyses of SNpc tissue from young adult and aged rats injected with rAAV2/2

GFP revealed a trend towards an age-related decrease in GFP mRNA, with the aged rat SNpc containing fivefold lower levels of GFP mRNA than the young adult SNpc (P = 0.109; Supplementary Figure S5c). In contrast, the SNpc of rats injected with rAAV2/9 contained equal levels of GFP mRNA between young adult and aged rats (P = 0.723; Supplementary Figure S5d). RNAscope *in situ* hybridization for GFP mRNA in the midbrain revealed a similar pattern, with decreased GFP mRNA puncta in the aged as compared to young adult rat following intranigral rAAV2/2 GFP injection, but not rAAV2/9 GFP injection (Supplementary Figure S5a,b). Decreased GFP mRNA in aged rats was also observed in RNAscope *in situ* hybridization with rAAV2/5 and LV (Supplementary Figures S5e,f), following the trends observed with rAAV2/2 (Supplementary Figure S5a,c) and a previous report demonstrating decreased GFP mRNA in

the aged ventral mesencephalon following transduction with rAAV2/5.[26] Together, these results suggest that levels of GFP mRNA are also decreased in cases where viral vectors display an age-related decrease in nigrostriatal transduction as assessed by GFP protein levels.

Experiment 2. Vector transgene expression levels in the striatonigral system and striatum following intrastriatal injections to the young adult and aged rat

Age-related decreases in exogenous GFP protein in the striatonigral system are observed following intrastriatal rAAV2/2, rAAV2/5, and rAAV2/9, but not LV injections. Similar to our assessment of the nigrostriatal system, the ability of intrastriatal vector injections to deliver exogenous GFP to the anterograde SNpr was measured by protein analyses in SNpr tissue (Supplementary Figures S1 and S2). Striatal injection of viral vectors expressing tropic factors are used to simultaneously provide exogenous protein to dopaminergic nigrostriatal terminals through local transgene expression and tropic factor secretion, and anterogradely deliver protein to the SN via the striatonigral pathway.[32,33] Aged rats displayed significantly lower levels of GFP protein as compared to young adult rats following injection with three of the four vector constructs (Figure 3). Similar to results following intranigral injections, rAAV2/2 displayed a 67% reduction in GFP expression ($P = 0.001$; Figure 3a) and rAAV2/5 displayed a 58% reduction in GFP expression ($P = 0.023$; Figure 3c) in the aged as compared to the young adult SNpr. However, unlike results with rAAV2/9, which displayed no age-related decrease in GFP protein expression following intranigral injections, following intrastriatal injections rAAV2/9 GFP expression was reduced by 55% in the aged SNpr as compared to the young

adult rat ($P = 0.001$; Figure 3b). In contrast, LV GFP was the sole viral vector resistant to the age-related decrease in transgene expression in the striatonigral system ($P = 0.402$; Figure 3d) despite displaying a deficiency in GFP expression in the aged as compared to young adult rat nigrostriatal system (Figure 1d). These results indicate that the aged rat striatonigral system is, in general, also relatively resistant to viral vector transduction when compared to the young adult rat. However, age-related decreases in transgene expression are unique to specific viral vectors and cannot be generalized across brain structures.

Age-related changes in striatonigral expression of GFP are not detectable by quantitation of GFP+ cells in the striatum. To assess the relationship between the number of transduced cells in the striatum and transgene expression in the striatonigral pathway, we quantified the total number of GFP+ cells within the striatum using unbiased stereology. No significant differences were observed in total numbers of striatal GFP+ cells following rAAV2/2 GFP ($P = 0.448$; Figure 4a), rAAV2/9 GFP ($P = 0.506$; Figure 4d), rAAV2/5 GFP ($P = 0.096$; Figure 4g), or LV GFP ($P = 0.762$; Figure 4j) injection into the aged versus young adult rat. As observed when we quantified total numbers of mesencephalic GFP+ cells, quantification of the total number of striatal GFP+ cells does not accurately reflect differences in transgene expression. Again, we quantified the ratio of GFP+ neurons to glia and did not see any differences with age as the vast majority (>98% for all vectors) of GFP+ cells displayed a neuronal phenotype (Supplementary Figure S6; Supplementary Table S1). Due to tissue processing requirements for striatal GFP+ cell quantitation, we were unable to perform direct protein quantification in the striatum. Therefore, to capture potential differences in levels of GFP expression within cells of the striatum, we quantified
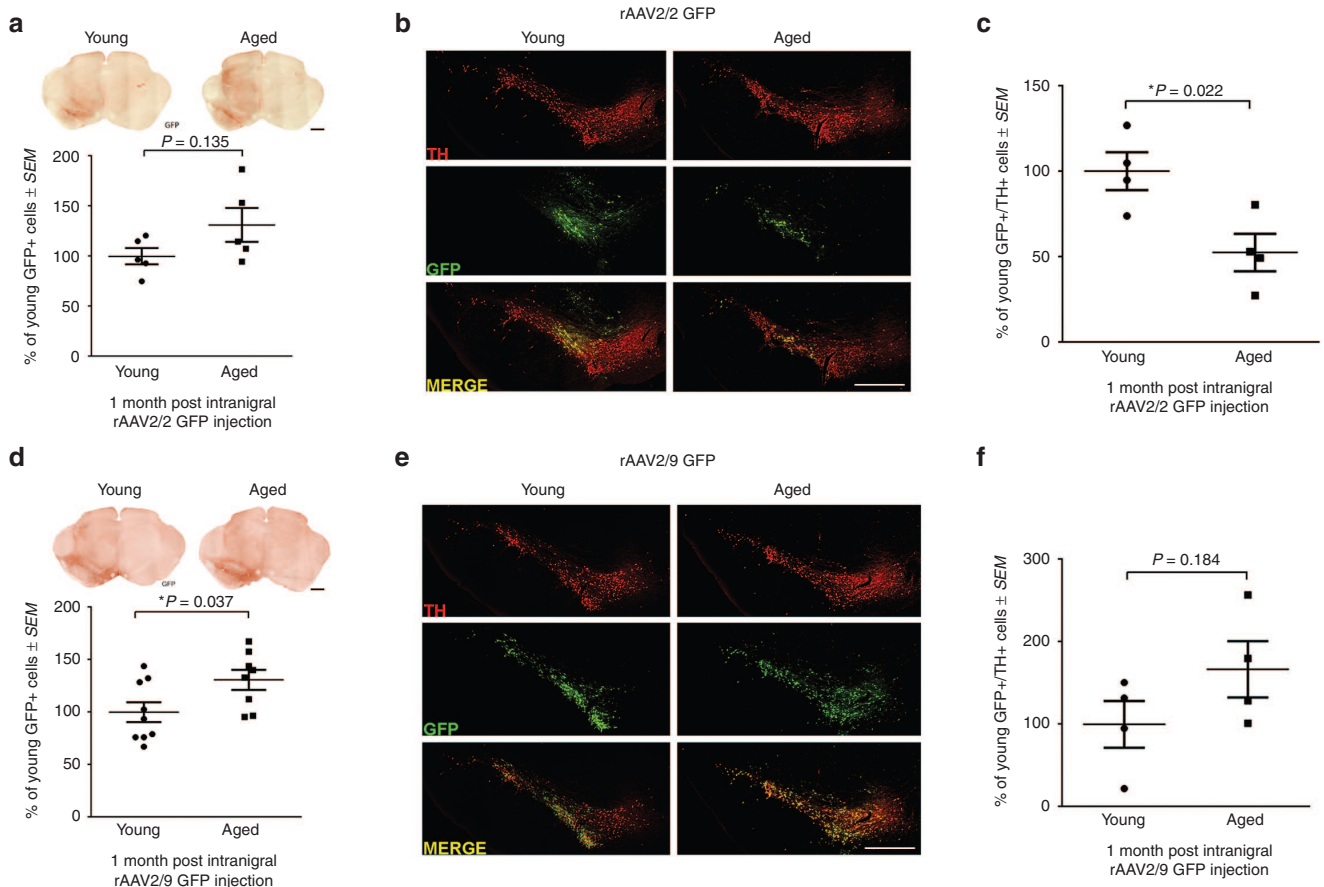
GFP immunoreactivity using near-infrared densitometry in the striatum (Figure 4b,e,h,k). Again, no significant differences were observed between ages with rAAV2/2 GFP ($P = 0.332$; Figure 4c), rAAV2/9 GFP ($P = 0.147$; Figure 4f), or LV GFP ($P = 0.758$; Figure 4l). However, advanced age resulted in a significant decrease in GFP immunoreactivity following intrastriatal rAAV2/5 GFP injection ($P = 0.021$; Figure 4i). Taken together, these results suggest that an age-related reduction in striatonigral transgene expression is difficult to detect at the level of the striatum following intrastriatal injection.

Evaluation of GFP mRNA expression following intrastriatal injection. RNAscope *in situ* hybridization was used to detect levels of GFP mRNA in striatal tissue one month after intrastriatal viral vector injection. Qualitative analyses failed to reveal any striking differences between young adult and aged rats in levels of GFP mRNA following intrastriatal injection with rAAV2/5, rAAV2/9 or LV (Supplementary Figure S7). However, striatal sections transduced using rAAV2/2 displayed an appreciable decrease in GFP mRNA in the aged as compared to young adult rat striatum (Supplementary Figure S7a). These results suggest, at least for rAAV2/2, that age-related deficiencies in GFP protein expression are related to an age-related decrease in GFP mRNA levels.[26,34]

Astrocytes display limited tropism for viral particles in the young adult and aged rat striatum. Previous studies report a doubling of astrocytes in the striatum in aged as compared to young adult rats.[35] We investigated the possibility that an increased astrocyte-to-neuron ratio impacted striatal neuron transduction efficiency in the aged brain due to astrocytes sequestering viral particles; a phenomenon that would not have been detected simply by looking at GFP expression since the activity of the CβA promoter is highly limited in astrocytes. We used a novel combination of RNAscope *in situ* hybridization for the viral CβA promoter[35] and immunohistochemistry for astrocytes (S100 calcium-binding protein B, S100B) or neurons (Neuronal Nuclei, Neu-N) to visualize the cellular location of viral particles in the transduced zone in the
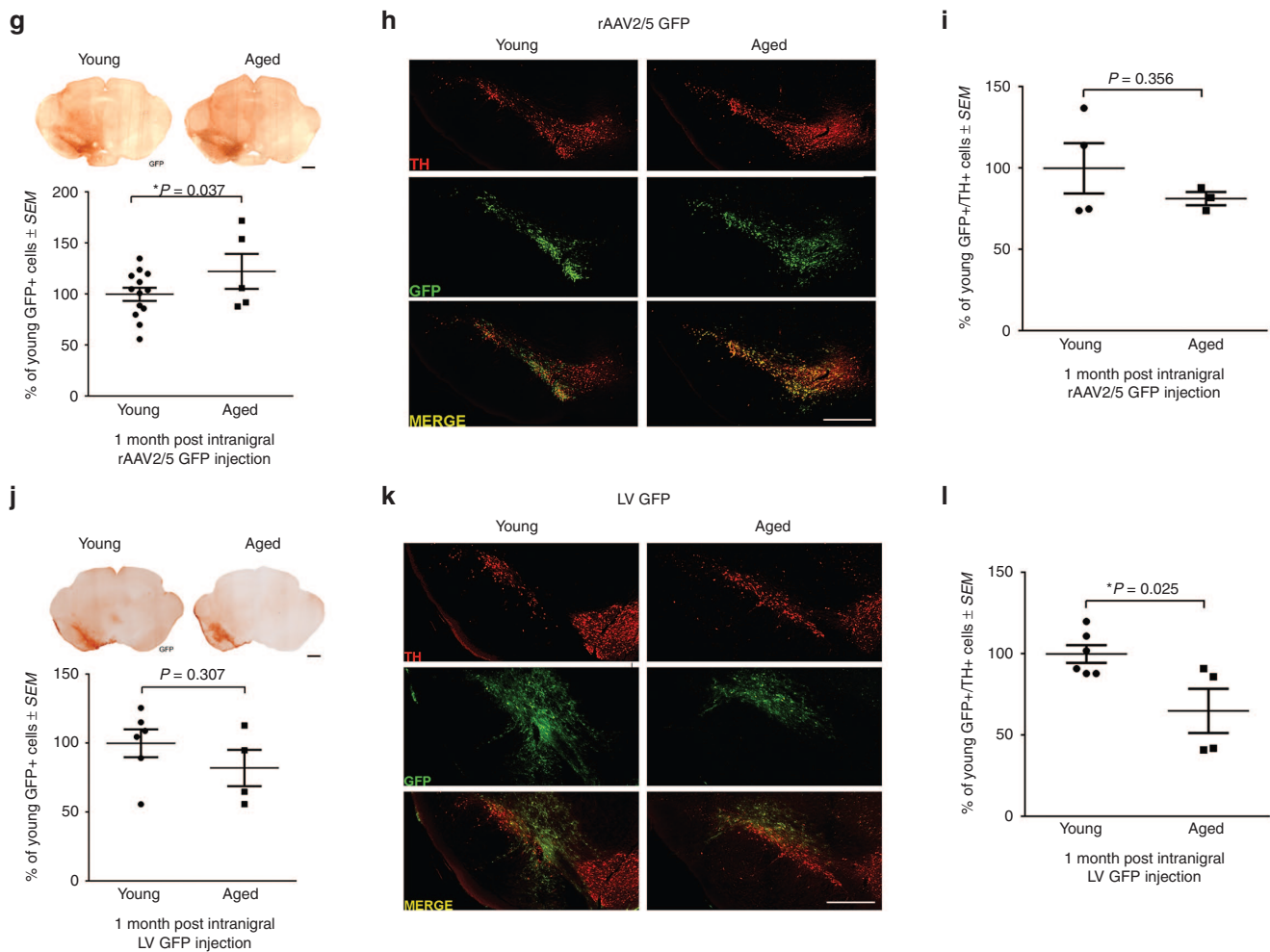

Figure 2 Quantitation of GFP-positive cells after intranigral injection does not consistently reveal age-related nigrostriatal transgene expression deficiencies. (**a,d,g,j**) Representative image and quantitation of total GFP+ cells in the midbrain of young adult (Young) and aged (Aged) rats following rAAV2/2, rAAV2/9, rAAV2/5, and LV GFP transduction, respectively. Scale bars = 1,000 μm. No significant differences ($P > 0.05$) were seen between young adult and aged rats in total GFP+ cells with (**a**) rAAV2/2 ($n = 5$/age), (**g**) rAAV2/5 ($n = 13$ young, 5 aged), and (**j**) LV ($n = 6$ young, 4 aged), but aged ($n = 9$) rats had significantly more GFP+ cells than young adult ($n = 8$) rats following (**d**) rAAV2/9 GFP transduction (*$P \leq 0.05$). (**b,e,h,k**) GFP expression within THir SNpc neurons in young adult and aged rats following rAAV2/2, rAAV2/9, rAAV2/5, and LV GFP transduction, respectively. Scale bars = 1,000 μm. (**c,f,i,l**) Quantitation of GFP+ cells colocalizing with TH+ cells in the SNpc following rAAV2/2, rAAV2/9, rAAV2/5, and LV GFP injection, respectively. Aged rats had significantly fewer (*$P \leq 0.05$) GFP+/TH+ cells than young adult rats following (**c**) rAAV2/2 and (**l**) LV injection ($n = 4$/age/vector). No significant differences ($P > 0.05$) were observed in the number of GFP+/TH+ cells in the SNpc between ages for (**f**) rAAV2/9 ($n = 4$/age) and (**i**) rAAV2/5 ($n = 4$ young, 3 aged). Values are expressed as the percent of the young cell counts ± SEM for each group. GFP, green fluorescent protein; GFP+, GFP immunoreactive; LV, lentivirus; TH+, tyrosine hydroxylase immunoreactive; rAAV, recombinant adeno-associated virus; SEM, standard error of the mean.

striatum. Despite previous evidence suggesting an increase in the population of astrocytes in the striatum with aging,[36] no qualitative increase in S100B astrocytes was observed in the aged compared to the young striatum. Further, in both the young adult and aged brain, for all vector constructs, viral genomes overwhelmingly colocalized with NeuN-immunoreactive neurons (Figure 5a–c and Figure 5g–i), indicating their presence within neurons, corresponding with our GFP-expression data (Supplementary Figures S4 and S6). Viral genomes within neurons appeared as numerous, dense CβA puncta. In contrast, viral genomes were rarely observed in astrocytes (Figure 5d–f and Figure 5j–l) and if observed, most often appeared as puncta representative of single viral genomes (Figure 5f,l). These results indicate that astrocytes in the aged striatum do not impact transduction efficiency via sequestration of viral particles. Further,

although use of astrocyte-specific promoters such as the GFAP promoter (rather than the CβA promoter) can limit gene expression to astrocytes,[37] our results suggest that rAAV2/2, rAAV2/5, rAAV2/9 and LV have limited tropism for astrocytes in the brain compared to neurons.

Experiment 3. Comparisons between rAAV pseudotype transgene expression in young adult and aged rats

rAAV2/9 delivers the most exogenous GFP protein to the nigrostriatal system of both young adult and aged rats. Nigrostriatal transgene expression following injection into the SNpc was assessed by quantifying GFP protein levels in the ipsilateral striatum (Supplementary Figure S1). Comparisons were made between all
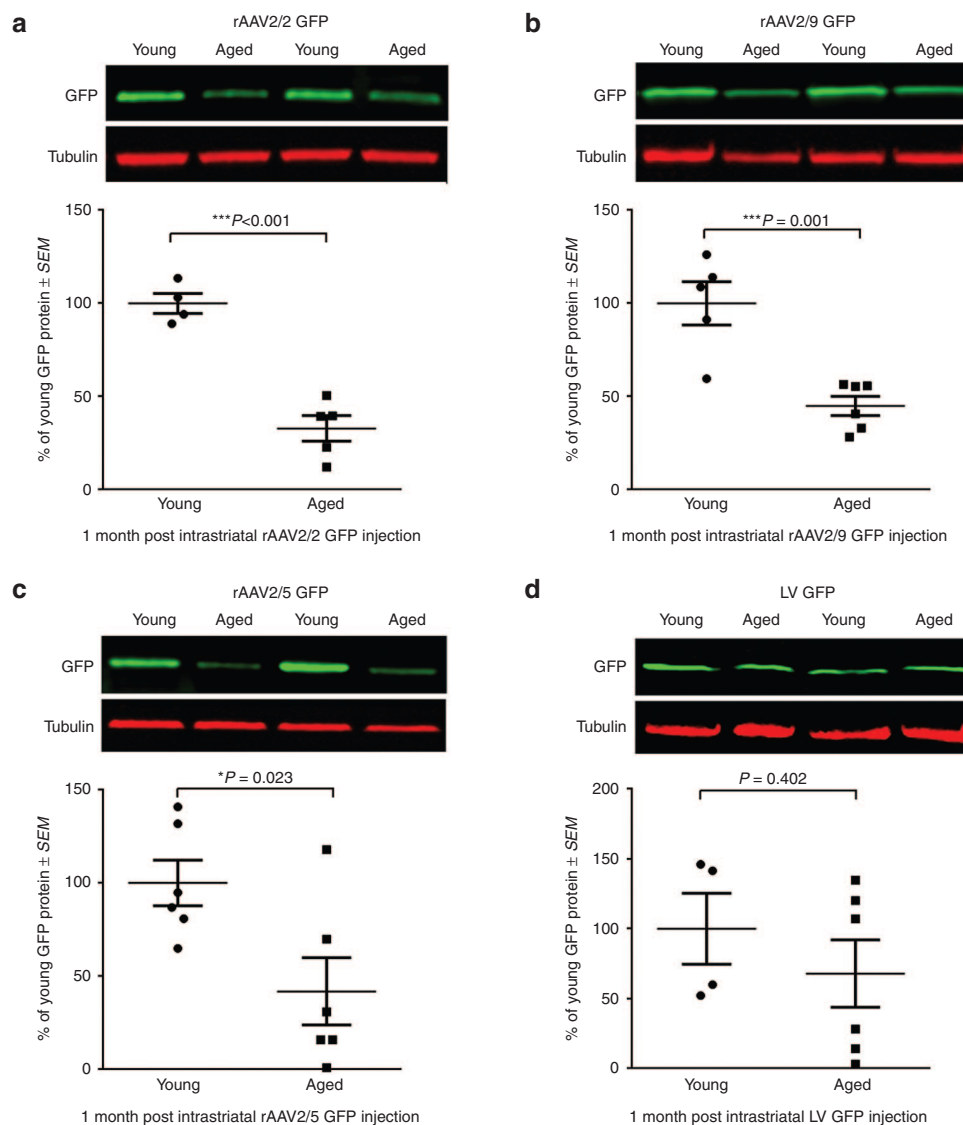

Figure 3 Viral vector-mediated expression of GFP is reduced in the aged striatonigral system with rAAV2/2, rAAV2/5, and rAAV2/9, but not LV. Representative Western blot and quantitation of GFP immunodetection in substantia nigra pars reticulata (SNpr) samples of young adult (Young) and aged (Aged) rats one month post-injection with (**a**) rAAV2/2 GFP, (**b**) rAAV2/9 GFP, (**c**) rAAV2/5 GFP, or (**d**) LV GFP. (**a**) Aged (*n* = 5) rats displayed significantly less GFP than young adult (*n* = 4) rats following rAAV2/2 GFP transduction (***$P \leq 0.001$). (**b**) Aged (*n* = 6) rats display decreased GFP levels in the SNpr as compared to young adult (*n* = 5) rats following rAAV2/9 GFP transduction (***$P \leq 0.001$). (**c**) Aged (*n* = 6) rats expressed significantly less GFP than young adult (*n* = 6) rats following rAAV2/5 GFP transduction (*$P \leq 0.05$). (**d**) Aged (*n* = 4) and young adult (*n* = 6) rats expressed equivalent GFP in the SNpr following LV GFP transduction ($P > 0.05$). Values are expressed as the percent of the young mean optical density scores, with GFP signal normalized to tubulin controls ± SEM for each group. GFP, green fluorescent protein; LV, lentivirus; rAAV, recombinant adeno-associated virus; SEM, standard error of the mean.

three rAAV pseudotypes injected with near-identical vector titers (rAAV2/2 = 1.9×10^{12} genomes/ml, rAAV2/5 = 2.0×10^{12} genomes/ml, and rAAV2/9 GFP at 2.0×10^{12} genomes/ml). LV was excluded from between-vector comparisons due to marked titer and transduction process differences. Injection of rAAV2/9 GFP into the SNpc resulted in significantly higher levels of GFP protein in the striatum of young adult ($F_{(2,5)}$ = 1232.34, $P < 0.001$; rAAV2/2 versus rAAV2/9, $P < 0.001$; rAAV2/5 versus rAAV2/9, $P < 0.001$) and aged brains ($F_{(2,3)}$ = 74.79, P = 0.003; rAAV2/2 versus rAAV2/9, P = 0.005; rAAV2/5 versus rAAV2/9, P = 0.005) (Figure 6a). rAAV2/5 nigrostriatal transduction efficiency was comparable with rAAV2/2 in aged rats, and although higher than rAAV2/2 in young rats, this did not reach statistical significance ($P > 0.05$). These results demonstrate that rAAV2/9 injections into both the young and aged SNpc result in the most efficient delivery of exogenous protein to nigrostriatal circuitry.

rAAV2/5 and rAAV2/9 transduce the greatest numbers of mesencephalic neurons in both young adult and aged rats. Following injection into the SNpc, comparisons were made between vectors in the number of total GFP+ cells throughout the midbrain (Figure 6b). Statistical differences were observed between vectors in both the young adult ($F_{(2,15)}$ = 5.23, P = 0.019) and the aged ($F_{(2,12)}$ = 11.80, P = 0.001) rats. Specifically, in the young adult midbrain, rAAV2/2 injection into the SNpc resulted in the lowest number of midbrain GFP+ cells with significantly fewer than rAAV2/9 (P = 0.018) but not rAAV2/5 (P = 0.165) (Figure 6b). In aged rats, a similar pattern was observed in which rAAV2/2 injections into the SNpc resulted in the fewest number of GFP+ cells in the mesencephalon, with significantly fewer

than rAAV2/5 (P = 0.008) and rAAV2/9 (P = 0.003). These results indicate that rAAV2/9 and rAAV2/5 yield the greatest number of transduced cells in the mesencephalon following SNpc injection, regardless of age.

rAAV2/5 and rAAV2/9 transduce the greatest numbers of TH+ SNpc neurons in young adult and aged rats. Statistical differences between vector constructs were also observed when SNpc neurons coexpressing TH and GFP were quantified (young adult, $F_{(2,9)}$ = 5.21, P = 0.031; aged, $F_{(2,8)}$ = 9.88, P = 0.007) (Figure 6c). In young adult rats, injection of rAAV2/5 into the SNpc resulted in the highest number of GFP+/TH+ SNpc neurons, with rAAV2/5 displaying significantly more GFP+/TH+ cells than rAAV2/2 (P = 0.035), but not rAAV2/9 (P = 0.172) (Figure 6c). In aged rats, the pattern was similar in that both rAAV2/5- and rAAV2/9-injected rats possessed significantly more GFP+/TH+ SNpc neurons than rAAV2/2 (rAAV2/5 versus rAAV2/2, P = 0.045; rAAV2/9 versus rAAV2/2, P = 0.008) (Figure 6c). Collectively, our results demonstrate that injections of both rAAV2/5 and rAAV2/9 result in the greatest numbers of transduced nigrostriatal dopamine neurons in young adult and aged rats compared to rAAV2/2. However, rAAV2/9 delivers the highest levels of GFP transgene to the young adult and aged nigrostriatal system by delivering the greatest levels of GFP transgene (≈35–63× greater) (Figure 6a).

rAAV2/9 delivers the most exogenous GFP protein to the striatonigral system of both young adult and aged rats. Comparisons in striatonigral transgene expression were made following intrastriatal injection of rAAV2/2 and rAAV2/9 in young adult and aged rats. As previously described, transgene expression in the striatonigral system was
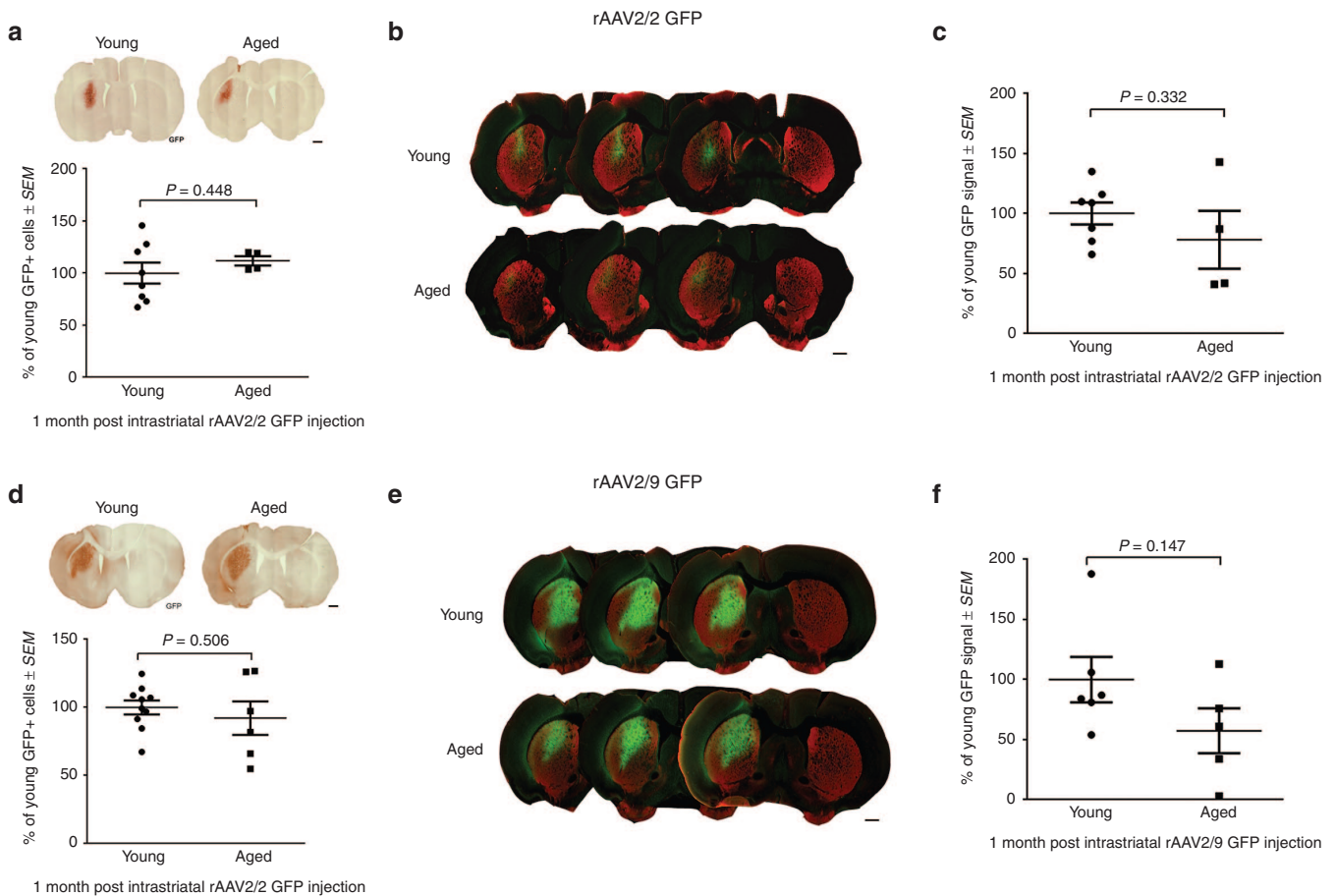
assessed by quantifying GFP levels in the SNpr following injection into the striatum (Supplementary Figures S1 and S2). rAAV2/5 was excluded from the GFP SNpr protein analyses due to lack of sample. The titers for the two rAAV pseudotypes injected into the striatum were relatively identical (rAAV2/2 = 1.9×10^{12} genomes/ml and rAAV2/9 GFP = 2.0×10^{12} genomes/ml). Similar to overall transduction efficiency measures in the nigrostriatal system, GFP levels in the SNpr resulting from intrastriatal rAAV2/9 injection were significantly greatly than SNpr GFP levels following intrastriatal rAAV2/2 injection in both the young adult (*P* = 0.003) and aged (*P* < 0.001) rat (Figure 7a). These results demonstrate that although advanced age negatively impacts the striatonigral transgene expression via rAAV2/9, rAAV2/9 remains the vector construct most capable of delivering high levels of exogenous protein to the striatonigral circuitry of both young adult and aged rats.

rAAV2/9 transduces the greatest number of striatal cells in both young adult and aged rats. Total numbers of GFP+ cells in the striatum were quantified after intrastriatal vector injection into young adult and aged rats and compared between vectors within each age group.

Multiple significant differences were observed in the young adult striatum using this outcome measure ($F_{(2,18)}$ = 69.89, *P* < 0.001) (Figure 7b). rAAV2/9 resulted in more GFP+ cells than rAAV2/2 (*P* < 0.001) and rAAV2/5 (*P* < 0.001). In addition, rAAV2/5 resulted in more GFP+ cells than rAAV2/2 (*P* = 0.006). A similar pattern was observed in the aged brain ($F_{(2,10)}$ = 12.54, *P* = 0.002) (Figure 7b) with rAAV2/9 injection resulting in significantly more GFP+ cells in the striatum compared to all other vectors (rAAV2/9 versus rAAV2/5, *P* = 0.025; rAAV2/9 versus rAAV2/2, *P* = 0.002). However, unlike results in young adults rats where intrastriatal injection of rAAV2/5 yielded more GFP+ neurons compared to rAAV2/2, in the aged brain intrastriatal rAAV2/5 resulted in statistically equivalent numbers as rAAV2/2 (*P* > 0.05). These results indicate that intrastriatal injection of rAAV2/9 yields the highest number of transduced cells in the striatum, regardless of age.

Following intrastriatal vector injections, GFP intensity in the striatum parallels GFP levels in the SNpr. Due to tissue processing requirements for striatal GFP+ cell quantification, we were unable to perform direct protein quantification in the striatum. To approximate
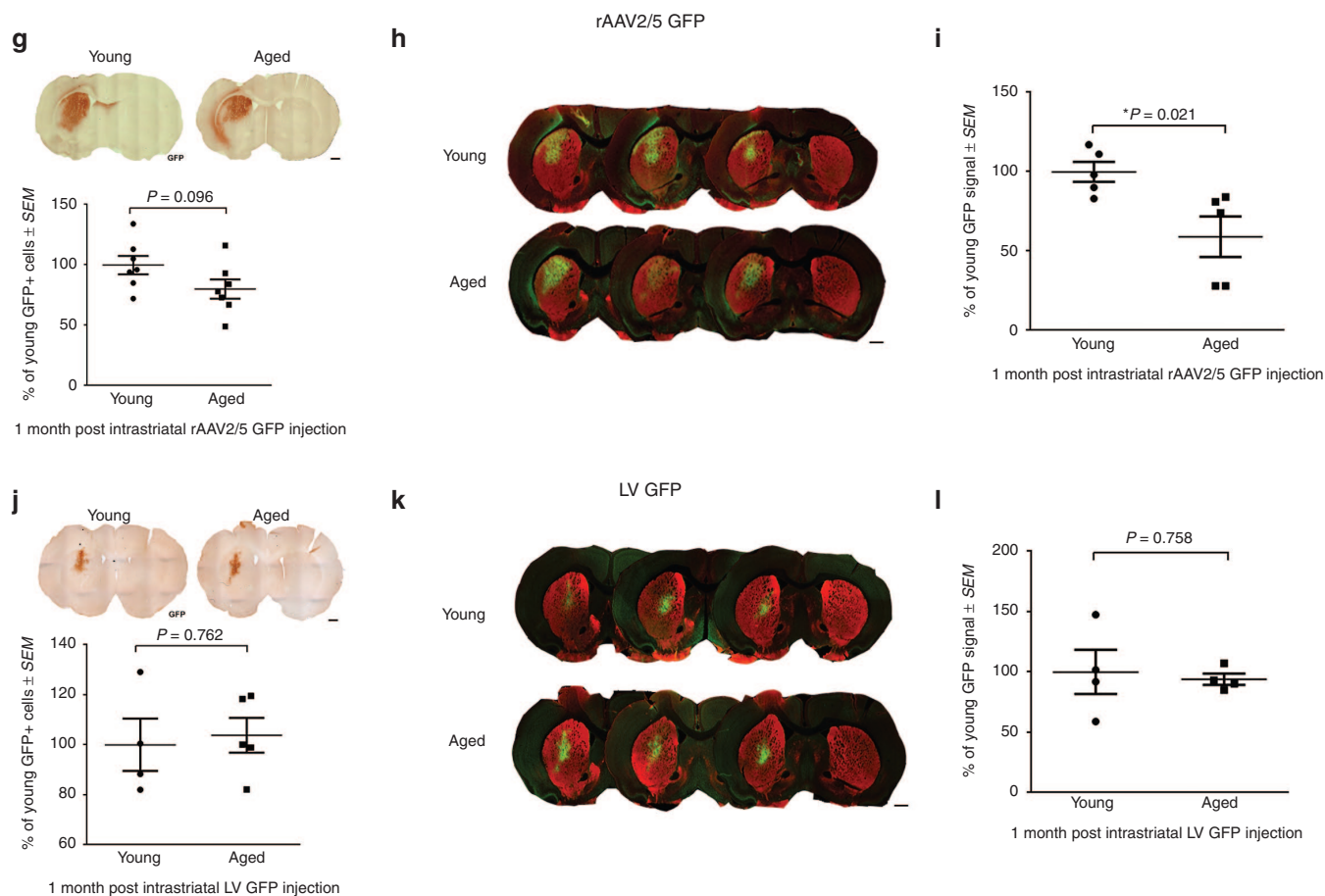

Figure 4 Quantitation of GFP-positive cells after intrastriatal injection does not reveal an age-related decrease in striatonigral transduction efficiency. (**a,d,g,j**) Representative image and quantitation of total GFP+ cells in the striatum of young adult (Young) and aged (Aged) rats following rAAV2/2, rAAV2/9, rAAV2/5, and LV GFP transduction, respectively. Scale bars = 1,000 µm. No significant differences (*P* > 0.05) were seen between young adult and aged rats in total GFP+ cells with (**a**) rAAV2/2 (*n* = 8 young, 4 aged), (**d**) rAAV2/9 (*n* = 10 young, 6 aged), (**g**) rAAV2/5 (*n* = 10 young, 6 aged), and (**j**) LV (*n* = 4 young, 5 aged). (**b,e,h,k**) GFP (green) and TH (red) expression detected using near-infrared imaging within the striatum of young adult and aged rats following rAAV2/2, rAAV2/9, rAAV2/5, and LV GFP transduction, respectively. Scale bars = 1,000 µm. (**c,f,i,l**) Quantitation of near-infrared GFP signal within the striatum following rAAV2/2, rAAV2/9, rAAV2/5, and LV GFP injection, respectively. Aged rats only displayed significantly decreased (*P ≤ 0.05) GFP signal following (**i**) rAAV2/5 GFP injection (*n* = 5/age), with no significant differences (*P* > 0.05) between ages following (**c**) rAAV2/2 (*n* = 7 young, 4 aged), (**f**) rAAV2/9 (*n* = 6 young, 5 aged), or (**l**) LV injection (*n* = 4/age). Values are expressed as the percent of the young GFP signal, normalized to background levels of staining in the cortex, ± SEM for each group. GFP, green fluorescent protein; LV, lentivirus; rAAV, recombinant adeno-associated virus; SEM, standard error of the mean; TH, tyrosine hydroxylase.
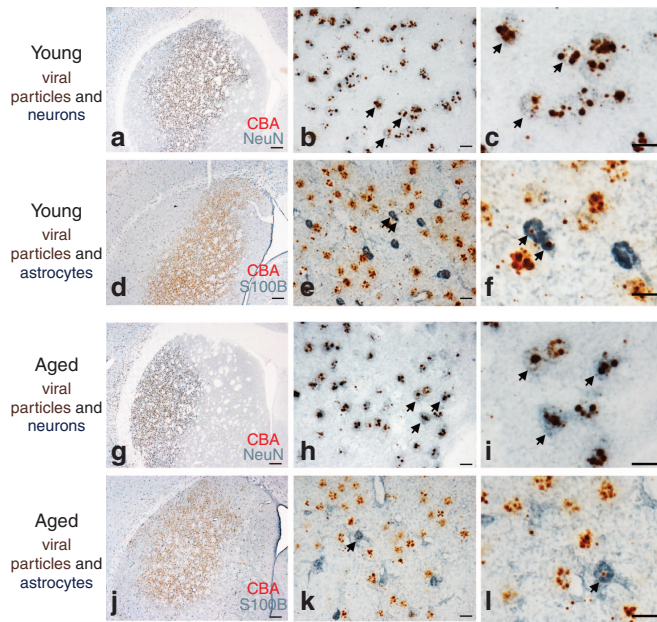
Figure 5 *In situ* hybridization combined with immunohistochemistry reveals viral particles located within neurons and largely absent within astrocytes in the striatum. (**a–c, g–i**) Representative image of RNAscope *in situ* hybridization of the CβA promoter of viral genomes (brown) and NeuN for neurons (blue) in young adult (**a–c**) or aged (**g–i**) rats 1 month postinjection of rAAV2/9 GFP in the striatum. (**d–f, j–l**) Representative image of RNAscope *in situ* hybridization for the CβA promoter of viral particles (brown) and S100B for astrocytes (blue) in young adult (**d–f**) or aged (**j–l**) rats one month postinjection of rAAV2/9 GFP in the striatum. Scale bars = 500 μm in lowest magnification panel, 25 μm in the intermediate and highest magnification panels. Arrows indicate areas of AAV genome colocalization within neurons or astrocytes.

striatal GFP protein delivery we analyzed near-infrared labeled GFP immunoreactive signal intensity in the striatum and made comparisons between vectors within age groups. Significant differences were observed in GFP signal intensity in the young adult ($F_{(2,12)}$ = 12.20, P = 0.001), but not the aged ($F_{(2,8)}$ = 2.97, P = 0.109) rat striatum (Figure 7c). As with SNpr GFP protein levels following intrastriatal injection, rAAV2/9 in the young adult brain resulted in the highest striatal GFP signal intensity compared to rAAV2/5 (P = 0.029) or rAAV2/2 (P = 0.001). GFP signal intensity also appeared highest following intrastriatal rAAV2/9 injection to aged rats, however this intensity was not significantly higher than those observed in aged rats with intrastriatal rAAV2/5 or rAAV2/2 injection. These results suggest that comparisons in striatonigral protein delivery quantified using direct protein measurements in the SNpr can generally be predicted using quantification of near-infrared signal intensity within the injected striatum. These results also suggest that in the young adult striatum, and to a lesser extent the aged striatum, rAAV2/9 results in the highest level of exogenous protein delivery.

rAAV2/9 results in the largest area of striatal transduction in both young adult and aged rats. The degree of vector spread away from the injection site can be a critical characteristic informing vector construct selection, particularly when targeting large structures like the striatum. To compare the area of striatal transduction between vectors, we measured the area of the GFP immunoreactivity in the striatum for each vector at both ages (Figure 7d). Significant differences were observed in the size of the GFP+ transduction area

in both the young adult ($F_{(2, 16)}$ = 44.56, P < 0.001) and aged ($F_{(2,13)}$ = 37.67, P < 0.001) rats. Similar patterns were observed for both young adult and aged rats, with the transduction area of rAAV2/9 being significantly greater than all other vectors (P < 0.001 for all comparisons in young adult and rAAV2/2 in aged, P = 0.002 for rAAV2/5 in aged). Similarly, in rats of both ages, the transduction area following rAAV2/5 injection was significantly greater than that achieved using intrastriatal rAAV2/2 (young adult, P = 0.005; aged, P = 0.001) (Figure 7d). Furthermore, no significant differences (P > 0.05) were observed in the transduction area of any viral construct for aged as compared to young adult rats (Figure 7d), supporting previous reports that an age-dependent diffusivity barrier is not the mechanism of the decreased transduction efficiency.[26] Collectively, our results using different vector constructs injected to the striatum indicate that despite reductions in transgene expression with advanced age, rAAV2/9 provides the greatest exogenous protein delivery and transduces the most striatal neurons compared to rAAV2/5 and rAAV2/2.

DISCUSSION

In the present study, we systematically investigated the generalizability of previous findings that advanced age appears to present a barrier to efficient viral vector transduction in the rat brain.[25,26] To this end, we injected rAAV2/2, rAAV2/5, rAAV2/9, and LV expressing GFP into the SNpc to transduce the nigrostriatal system or into the striatum to transduce the striatonigral system. We prioritized measurements of GFP protein in anterograde structures as the primary readout of transgene expression based on the ability of this outcome measure to provide a simultaneous readout of protein delivery and pathway specificity. We also used multiple additional outcome measures to quantify transduced neurons, measure GFP mRNA, and evaluate vector spread. In general, we observe a decrease in exogenous transgene expression following injection of most of the viral vectors tested in the nigrostriatal and striatonigral systems. Importantly, age-related decreases in GFP expression are not identical when targeting nigrostriatal versus striatonigral pathways. Specifically, following injections into the aged SNpc, transgene expression mediated by rAAV2/2, rAAV2/5, and LV is significantly compromised whereas rAAV2/9-mediated transduction is not negatively impacted by advanced age (Figure 1). Transgene expression in the aged striatonigral system is similarly compromised for all the rAAV pseudotypes; however, GFP expression mediated by LV is not deficient with age (Figure 3). For both neural pathways, however, rAAV2/9 emerged as the viral construct capable of delivering the most exogenous GFP protein to both young adult and aged rats, despite the decrease of transgene expression observed in the striatonigral system (Figures 6 and 7). For transduction of the greatest number of nigrostriatal dopamine neurons, both rAAV2/5 and rAAV2/9 were superior to the other vector constructs, regardless of age. These results provide evidence that age-related decreases in transgene expression are specific to viral construct and cannot be generalized across brain structures.

Another important finding of our study is that age-related transgene decreases (reduced GFP expression) in both neural pathways were not appreciable using quantitation of GFP+ cells. Unbiased stereological counts of GFP+ cells at the injection site did not reveal significant deficits in aged rats following SNpc or striatal injections, and differences in GFP protein delivery between vector constructs were not always detectable using GFP+ cell counts. This could be the result of multiple factors. For instance, the binary nature of cell counts (GFP+ "yes" or "no") could conceal differences in per-cell

Reduced transgene expression in aged striatum and substantia nigra
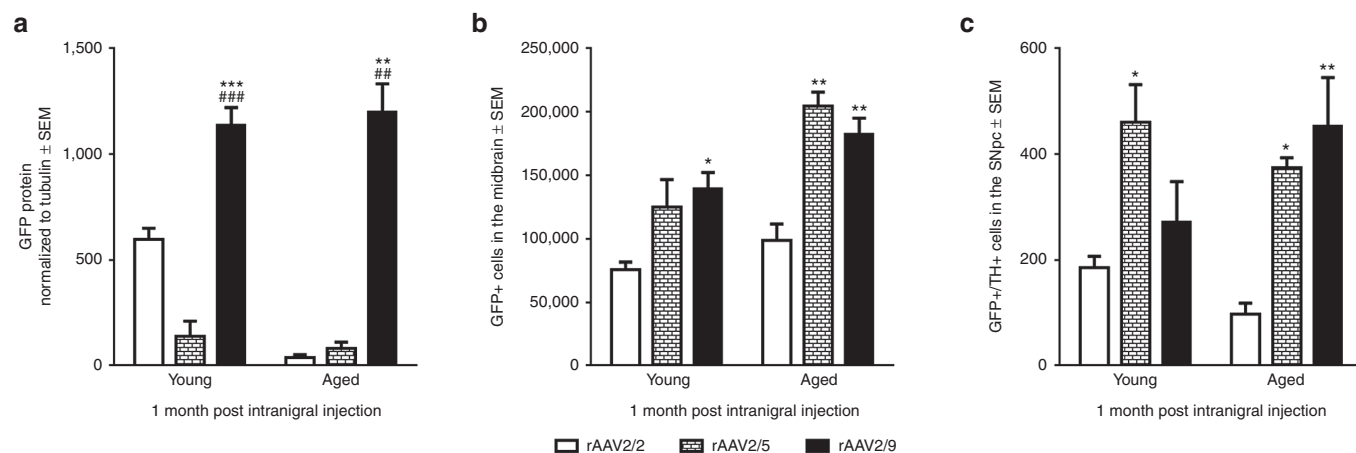NK Polinski et al.

10

Figure 6 Comparisons between rAAV2/2, rAAV2/5, and rAAV2/9 in the young adult (Young) or aged (Aged) rat nigrostriatal system. (**a**) Quantitation of Western blot GFP immunodetection in striatal tissue after intranigral injection of rAAV pseudotypes in the young adult and aged rat. (**b**) Quantitation of total numbers of GFP+ cells in the young adult and aged rat midbrain following injection of rAAV2/2 GFP, rAAV2/5 GFP, or rAAV2/9 GFP into the substantia nigra pars compacta (SNpc). (**c**) Quantitation of the number of cells coexpressing GFP and tyrosine hydroxylase (TH) in the young adult and aged rat SNpc following SNpc injection. Data is expressed as mean values ± SEM for each group. Statistical differences between vectors in each age group are depicted as follows—comparisons against rAAV2/2: *$P \leq 0.05$, **$P \leq 0.01$, ***$P \leq 0.001$; comparisons against rAAV2/5: #$P \leq 0.05$, ##$P \leq 0.01$, ###$P \leq 0.001$. GFP, green fluorescent protein; GFP+, GFP immunoreactive; rAAV, recombinant adeno-associated virus; SEM, standard error of the mean; TH+, tyrosine hydroxylase immunoreactive.

multiplicity of infection (MOI) that could account for the observed decrease in GFP protein expression with advanced age. This possibility is corroborated by a previous report describing decreased immunoreactivity in individually-transduced aged neurons following rAAV2/2 transduction of the aged and young adult rat septum.[25] Further, injections into the SNpc result in the transduction of both nigral dopamine neurons as well as other nondopaminergic neurons in the SN and surrounding ventral mesencephalon. As a result, counts of GFP+ cells in the mesencephalon could provide an inaccurate picture of the relative numbers of GFP+/TH+ SNpc neurons. Quantitation of GFP+ cells is the most common outcome measure used to report transduction efficiency.[8,22,23,30,31,38,39] Our findings confirm previous reports in which rAAV2/9 generally results in the greatest number of GFP+ cells, followed by rAAV2/5 and lastly rAAV2/2.[8,14,16] Further, our results mirror those in which counts of GFP+/TH+ nigral neurons are greater following injection of rAAV2/5 into the SNpc compared to rAAV2/2.[31] However, despite the fact that both rAAV2/9 and rAAV2/5 resulted in similar numbers of transduced SNpc neurons, this only partially predicted GFP protein expression. These results indicate that caution should be exercised when using counts of GFP+ cells or GFP+/TH+ neurons to assess efficiency of transgene expression.

The mechanism dictating reduced transgene expression in the aged brain is unclear. Previous studies have reported a doubling of astrocytes in the striatum of aged as compared to young adult rats.[36] To investigate the possibility that reduced transgene expression in the aged striatum is due to increased numbers of astrocytes sequestering viral genomes from neurons, we analyzed the number of viral particles within neurons vs. astrocytes. We did not observe any appreciable qualitative differences in the number of astrocytes in the young adult versus aged rat striatum. Further, regardless of vector construct, viral genomes were overwhelmingly observed within neurons and rarely observed within astrocytes. Taken together, these results indicate that the mechanism of the age-related decrease in striatal AAV transgene expression is not due to astrocyte sequestration of viral particles.

The fact that age-related decreases in exogenous transgene expression in the brain are not universal eliminates potential ubiquitous age-related impairments such as axonal transport deficits as a possible mechanism. Furthermore, age-related axonal transport deficiencies are unlikely to be involved due to the fact that untagged GFP is not believed to be actively transported along axons but, rather, freely diffuses through the cell.[40] Our present and past data[26] demonstrating that vector spread is unaffected by aging also suggest that reduced diffusivity in the aged brain is not a factor. Instead, we suggest that capsid-mediated differences are implicated in the observed transduction deficiencies. We point to the fact that rAAV2/2 and rAAV2/5 transduction is deficient in the aged nigrostriatal system whereas rAAV2/9 is not. The viral genome of these three rAAV pseudotypes is identical, and the sole difference between them is the capsid used—implicating capsid-related steps of transduction in the age-related deficiencies for rAAV.[41] One capsid-related step of transduction that could be deficient with age is receptor-mediated endocytosis. Each vector pseudotype uses a distinct set of receptors for endocytosis (main receptors: rAAV2, heparin sulfate proteoglycan[42,43]; rAAV5, 2,3-linked sialic acid[44]; rAAV9, N-linked galactose[45,46]; VSV-G LV, phosphatidylserine[47,48]) and a precedence exists for a decrease in some receptors in the aged as compared to young adult brain.[49,50] Furthermore, the qualitative and quantitative deficits in GFP mRNA we observed parallel protein deficits, further implicating steps of transduction prior to protein synthesis in our observed transduction deficiencies.[26,34,41] Additional experiments will be required to determine the cause of the age-related transduction deficiencies in an effort to circumvent deficiencies and improve transduction in the aged brain.

Characterizing the efficiency of transduction between young adult and aged rats is important when using viral vectors as research tools in studies of aging or age-related disease. For instance, previous studies in our lab attempted to overexpress human wildtype alpha-synuclein (α-syn) using rAAV2/5 injected into the young adult and aged rat SNpc in order to investigate mechanisms of α-syn-related toxicity in the aged brain environment.[7] Unbiased
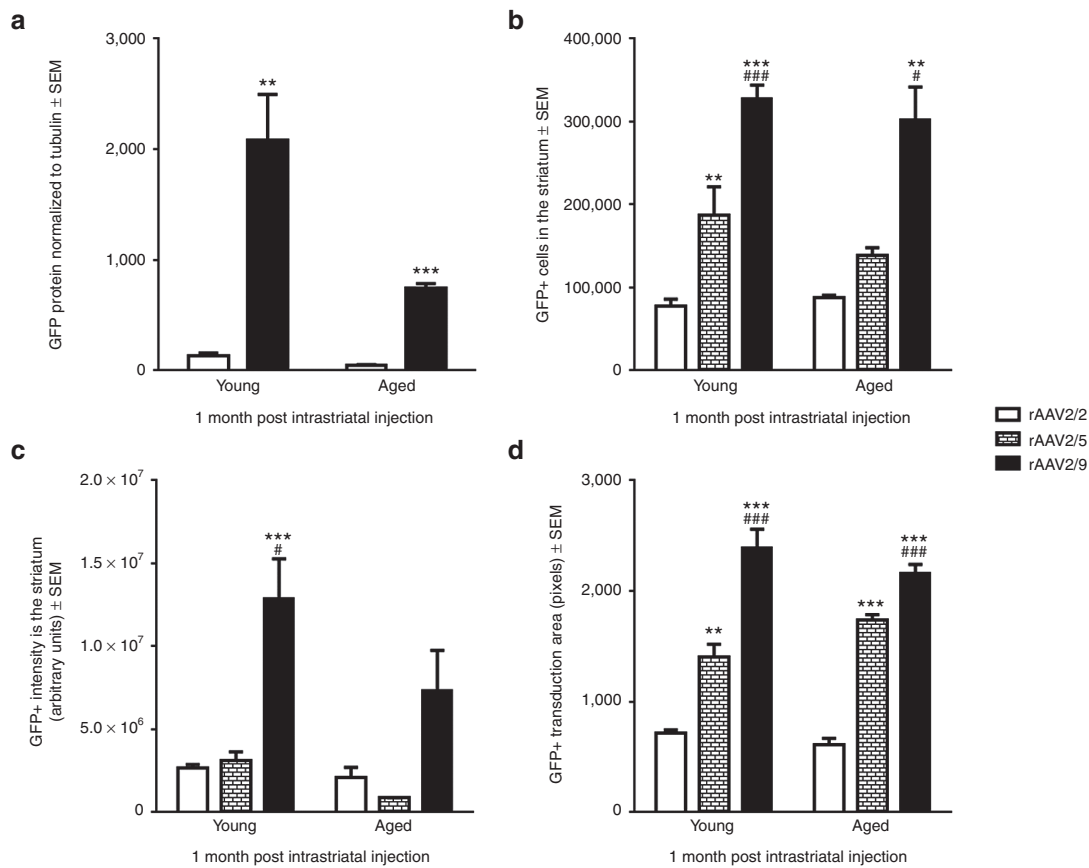
Reduced transgene expression in aged striatum and substantia nigra
NK Polinski et al.

11

Figure 7 Comparisons between rAAV2/2, rAAV2/5, and rAAV2/9 in the young adult (Young) or aged (Aged) rat striatonigral system. (**a**) Quantitation of Western blot GFP immunodetection in SN pars reticulata (SNpr) tissue after intrastriatal injection of rAAV2/2 and rAAV2/9 in the young adult and aged rat. rAAV2/5 was excluded in this Western blot due to lack of tissue. (**b**) Quantitation of total numbers of GFP+ cells in the striatum of young adult and aged rats following injection of rAAV2/2, rAAV2/5, and rAAV2/9. (**c**) Quantitation of GFP signal following rAAV2/2, rAAV2/5, or rAAV2/9 injection in the striatum, as detected by near-infrared immunostaining. (**d**) Quantitation of the area of GFP expression (GFP+ transduction area) in the striatum as calculated by the LI-COR Image Studio 3.1 software. Data is expressed as mean values ± SEM for each group. Statistical differences between vectors in each age group are depicted as follows—comparisons against rAAV2/2: *$P \leq 0.05$, **$P \leq 0.01$, ***$P \leq 0.001$; comparisons against rAAV2/5: #$P \leq 0.05$, ##$P \leq 0.01$, ###$P \leq 0.001$. GFP, green fluorescent protein; GFP+, GFP immunoreactive; rAAV, recombinant adeno-associated virus; SEM, standard error of the mean.

stereological estimates in the SNpc revealed equivalent neuronal loss between young adult and aged rats. Without the additional examination of α-syn protein expression, these results could have been misinterpreted to suggest that aging does not impact α-syn-mediated toxicity. However, measurements of exogenous human wildtype α-syn in the striatum revealed substantially less rAAV2/5-delivered α-syn protein in the aged as compared to young adult rat striatum.[7] With this information, our results suggest the opposite conclusion—that aging exacerbates α-syn toxicity. Importantly, any paradigm utilizing viral vector-delivered protein to make comparisons between the aged and young adult brain should verify equivalent expression levels in their neural system of interest.

The striatum is the structure most often targeted in PD gene therapy clinical trials[3,13,16,28] as this approach can be used to simultaneously provide exogenous protein to dopaminergic nigrostriatal terminals and anterogradely deliver protein to the SN via the striatonigral pathway.[32,33] In our laboratory, we have successfully used intrastriatal transduction of the young adult rat striatum with a trophic factor (pleiotrophin) to protect the nigrostriatal dopamine system from 6-hydroxydopamine toxicity.[51] Our present results suggest that despite the age-related deficiency in transduction observed, intrastriatal rAAV2/9 may be optimally suited to deliver the greatest amount of trophic factor to the aged striatonigral system (as well as the aged

nigrostriatal system). However, it is important to note that multiple concerns underlie the use of rAAV9, such as an elicitation of an adaptive immune response and subsequent neuronal loss that has been associated with this vector when delivering potentially antigenic proteins.[52,53] Furthermore, the ability of rAAV9 to cross the blood–brain barrier and possibly escape the brain after intraparenchymal injection may also be an important consideration.[54] It is possible that altering the promoter, transgene, vector backbone, or titer may combat some of these issues and improve the safety profile of the rAAV9 for use in gene therapy for neurodegenerative diseases.[53,54]

Gene therapy clinical trials for PD use rAAV2/2 or LV for transduction of the aged striatum.[3,13,16,28] Our results demonstrate that striatonigral rAAV2/2-mediated transgene expresssion is markedly reduced with aging and is less efficient compared to rAAV2/5 and rAAV2/9. Additional studies should be conducted to identify the optimal vector construct for safe and efficient transgene delivery to the aged parkinsonian brain. Ideally, studies should be extended to also address whether expression of other transgenes is impacted by aging, especially those encoding biologically-relevant or secretable proteins such as glial cell line-derived neurotrophic factor. The impact of age on viral vector transduction efficiency is an extremely important consideration as efficient transduction will be required for functionally-meaningful gene therapy for age-related neurodegenerative diseases.

MATERIALS AND METHODS

Experimental overview

Cohorts of Fischer 344 (F344) rats, 10 young adult (3 months old) and 10 aged (20 months old) per cohort, were unilaterally injected with rAAV2/5, rAAV2/2, rAAV2/9, or VSV-G pseudotyped LV (LV) expressing GFP into the SNpc (nigrostriatal transduction) or into the striatum (striatonigral transduction) (Supplementary Figure S1). All cohorts were sacrificed 1 month postinjection. In general, the anterograde structure of the system—striatum for nigrostriatal system and SN pars reticulata (SNpr) for striatonigral system—was used for Western blot analysis of GFP protein and the brain region containing the injected structure was used for immunohistochemical staining and *in situ* hybridization (or qPCR for rAAV2/2 and rAAV2/9 injections in the SNpc). We chose to perform transduced cell quantitation in the injected structure and transgene expression in the anterograde structure protein to allow for the proper quality control of injection placement that is made possible by immunohistochemical examination of transduction area *in situ*. Outliers were removed if they displayed a misplaced injection or met the criteria for exclusion through the ADAM outlier method[55] and were not included in any outcome measure in this study (see Supplementary Table S2 for detailed information on outlier removal for each cohort).

Animals

Male, Fischer344 rats (National Institute on Aging, Bethesda, MD) 3 months of age (*n* = 98) and 20 months of age (*n* = 102) were used in this study. All animals were given food and water *ad libitum* and housed in 12 hours reverse light–dark cycle conditions in the Van Andel Research Institute vivarium, which is fully Association for Assessment and Accreditation of Laboratory Animal Care (AAALAC) approved. All procedures were conducted in accordance with guidelines set by the Institutional Animal Care and Use Committee of Michigan State University.

Viral vectors

All rAAV viral vector constructs were purchased from the University of Florida Powell Gene Therapy Center Vector Core (University of Florida, Gainesville, FL). Plasmid and vector production were completed as previously described.[56–58] For all vectors, expression of the transgene was driven by the chicken beta actin/cytomegalovirus enhancer (CβA/CMV) promoter hybrid. For rAAV production, humanized GFP was inserted into an AAV plasmid backbone containing AAV2 inverted terminal repeats and was packaged into AAV5, AAV2, or AAV9 capsids via cotransfection with a plasmid containing *rep* and *cap* genes and adenovirus helper functions. Particles were purified using iodixanol gradients followed by column chromatography, and dotblot was used to determine vector titer.[59] For LV production, the same GFP expression cassette was inserted into an LV transfer vector and triple transfections were performed into HEK-293 cells with the LV transfer vector and LV helper plasmids and LV was purified from cellular media by ultracentrifugation.[56] The vector titers used in this study were the following: rAAV2/2 GFP at 1.9×10^{12} vector genomes (vg)/ml, rAAV2/5 GFP 2.0×10^{12} vg/ml, rAAV2/9 GFP at 2.0×10^{12} vg/ml, LV in the striatum at 2.0×10^{7} vg/ml, and LV in the SNpc at 5.0×10^{7} vg/ml. Due to the unexpected attrition of many aged rats following the first set of nigral and striatal rAAV2/5 injections, we performed additional vector injections using an additional stock of rAAV2/5 GFP that despite best titer adjustment efforts was slightly lower (1.2×10^{12} vg/ml, not 2.0×10^{12} vg/ml). Comparisons within vector type between young and aged rats were made in rats injected with the identical titers and comparisons between vector constructs were only made in rats injected with a vector titer between $1.9–2.0 \times 10^{12}$ vg/ml, excluding the rats injected with rAAV2/5 GFP at the 1.2×10^{12} vg/ml titer. All surfaces (syringes, pipettes, and microcentrifuge tubes) were coated in SigmaCote (Sigma-Aldrich, St. Louis, MO) prior to coming in contact with the virus to minimize binding of viral particles.[58]

Viral vector injections

All surgical procedures were performed under isofluorane anesthesia (5% in O_2 for induction and 2% in O_2 for maintenance). Rats were placed in a stereotaxic frame and a Hamilton syringe fitted with a glass capillary needle (Hamilton Gas Tight syringe 80,000, 26s/2″ needle; Hamilton, Reno, NV; coated in SigmaCote) was used for injections. For intranigral injections of GFP-expressing viruses, two 2 μl injections were injected in the left SNpc at coordinates (from dura) AP −5.3 mm, ML +2.0 mm, DV −7.2 mm, and AP −6.0 mm, ML +2.0 mm, and DV −7.2 mm as previously described.[30,33] For intrastriatal injections of GFP-expressing viruses, one 2 μl injection was injected in the left striatum at coordinates (from dura) AP +0.0 mm, ML +2.7 mm, DV −4.0 mm in the young adult and adjusted to AP +0.0 mm, ML +3.0 mm, DV −4.0 mm in the aged rat.[29] The glass needle was lowered to the site and vector injection began immediately at a rate of 0.5 μl/minute and remained in place after the injection for an additional 5 minutes before retraction.

Euthanasia and tissue preparation

All rats were sacrificed 1 month postinjection. Rats were deeply anesthetized (60 mg/kg, pentobarbital, i.p.) and perfused intracardially with 0.9% saline containing 1 ml/10,000 USP heparin, followed by ice cold 0.9% saline. Rat brains were immediately removed and hemisected in the coronal plane at approximately AP −2.64 mm. In rats that were injected in the SNpc, rostral tissue was processed for microdissections and caudal tissue was processed for immunohistochemistry. In rats that were injected in the striatum with GFP-expressing viral vectors, rostral tissue was processed for immunohistochemistry, and caudal tissue was processed for microdissections.

Microdissections of striatum and SNpr

After brain removal, portions of the brains designated for microdissection were chilled in ice-cold saline for 2 minutes and immediately microdissected (striatal tissue) or flash frozen in 2-methylbutane on dry ice and stored at −80 °C (SNpc tissue).

Striatal tissue for protein analyses (SN-injected GFP vectors)

Following 2 minutes incubation in ice-cold saline to firm and chill the tissue, 2 mm coronal slabs were blocked from each brain utilizing an aluminum brain blocker (Zivic, Pittsburg, PA). Striatal tissue from both hemispheres was microdissected with a 2 mm tissue punch on a petri dish over ice. Frozen dissected structures were placed in prechilled microcentrifuge tubes and stored at −80 °C.

SNpc tissue for RNA analyses (SN-injected rAAV2/2 GFP and rAAV2/9 GFP)

All surfaces and instruments were cleaned with RNase Away (Invitrogen, Carlsbad, CA) when collecting tissue for RNA analyses. Brains were warmed from −80 °C to −15 °C for 1 hour before use. Brains were mounted onto metal chucks with Tissue-Tek O.C.T. (VWR, Vatavia, IL) before being moved to a −20 °C cryostat for sectioning. Tissue was sectioned until the SNpc became visible. Punches were taken from the rostral face of the brain structures once the structure was definitively apparent to ensure precision. A 2×1 mm oval punch of tissue was taken of the SNpc for GFP RNA analyses using a custom punch. Tisue punches were placed in separate prefrozen RNase-free microcentrifuge tubes containing TRIzol Reagent (Invitrogen, Grand Island, NY) and tissue was homogenized with a pestle before storage. Samples were stored at −80 °C until time of assay.

SNpr tissue for protein analyses (STR-injected GFP vectors)

Brains were transferred from −80 °C to −20 °C before microdissections. Brains were mounted on metal chucks with Tissue-Tek O.C.T. (VWR, Vatavia, IL) before being mounted in the cryostat at −15 °C. Tissue was sectioned until the level of the SNpr and punches were taken from the rostral face of the brain structures once the structure was definitively apparent to ensure precision. While it is possible that GFP expression in the striatum or in the SNpr may reflect some level of retrograde transport from the SNpc and striatal injection sites, respectively, the majority of GFP protein detected in these structures likely represents transgene levels within the nigrostriatal (SNpc injections) and striatonigral circuitry (striatal injections). A 2×1 mm oval punch was taken of the region immediately ventral to the SNpc to collect the SNpr using a custom tissue punch. Tissue punches were placed in separate prefrozen microcentrifuge tubes and stored at −80 °C until time of analysis. SNpr punches were overwhelmingly comprised of tissue from the SNpr with precision of the punch verified by sectioning and immunostaining for tyrosine hydroxylase (Supplementary Figure S2).

Western blot

Striatal samples for western blot analyses were homogenized on ice in RIPA Lysis Buffer System (Santa Cruz, Dallas, TX) and SNpr samples for western blot analyses were homogenized on ice in 2% SDS. Total protein

concentration was determined by the Bradford protein assay. Samples were prepared at 30 ng total protein samples. Western blot protocol was completed as previously described.[33] Samples were electrophoresed using SDS-PAGE gels and transferred to Immobilon-FL membranes (Millipore, Bedford, MA). Membranes were incubated in primary GFP antisera (Abcam, Cambridge, MA; rabbit polyclonal IgG, Ab290, 1:1,000) with β-tubulin antisera (Cell Signaling, Danvers, MA; mouse monoclonal IgG, 4466, 1:1,000) overnight. IRDye800 conjugated goat anti-rabbit (LI-COR Biosciences; 926–32211, 1:15,000) and IRDye680 conjugated goat anti-mouse (LI-COR Biosciences, 926–68020, 1:15,000) were used as secondary antibodies. All antibody dilutions were made in LI-COR compatible StartingBlock T20 (TBS) Blocking Buffer (Thermo Scientific, Waltham, MA). Multiplexed signal intensities were imaged with both 700 and 800 nm channels in a single scan with a resolution of 169 μm using the Odyssey infrared image system (LI-COR Biosciences). Reported integrated intensity measurements of GFP expression were normalized according to the corresponding β-tubulin densitometry measurements as β-tubulin protein levels do not change with age.[60] The representative image was produced in Photoshop 7.0 (San Jose, CA).

Immunohistochemistry

The portion of the brains designated for immunohistochemistry were postfixed in 4% paraformaldehyde (Electron Microscopy Sciences, Hatfield, PA) in 0.1M PO_4 buffer for seven days. After this period they were transferred to 30% sucrose in 0.1M PO_4 buffer until saturated. Brains were frozen on dry ice and tissue was collected as a 1 in 6 series in a 24-well plate. The first five sections were taken at a 40 μm thickness with the remaining well housing two sections taken at a 20 μm thickness using a sliding microtome. Every sixth section was processed for immunohistochemistry using the free floating method (or every twelfth section in the case of glial immunohistochemistry).

Immunohistochemistry

Tissue sections were rinsed in Tris buffer and quenched in 0.3% H_2O_2 for 15 minutes, blocked in 10% normal goat serum for 1 hour, and incubated in primary antisera (TH: Millipore MAB318, mouse anti-TH, 1:4,000; GFP: Abcam Ab290, rabbit anti-GFP, 1:100,000) overnight at 4 °C. Following primary incubation, TH-labeled sections were incubated in biotinylated secondary antisera against mouse IgG (Vector BA-2001, biotinylated horse anti-mouse IgG, rat absorbed, 1:1,000) and GFP-labeled sections were incubated in biotinylated secondary antisera against rabbit IgG (Millipore AP132b, goat anti-rabbit IgG, 1:500) for 2 hours at room temperature, followed by Vector ABC detection kit using horseradish peroxidase (Vector Laboratories, Burlingame, CA). Antibody labeling was visualized by exposure to 0.5 mg/ml 3,3′ diaminobenzidine and 0.03% H_2O_2 in Tris buffer. Sections were mounted on subbed slides, dehydrated via ascending ethanol washes, cleared with xylene, and coverslipped with Cytoseal. Images were taken on a Nikon Eclipse 90i microscope with a QICAM camera (QImaging, Surrey, British Colombia, Canada). Figures were produced in Photoshop 7.0 (Adobe, San Jose, CA), with brightness, saturation, and sharpness adjusted only as needed to best replicate the immunostaining as viewed directly under the microscope.

TH and GFP double label immunofluorescence

Sections were blocked in 10% normal donkey serum for 1 hour and subsequently transferred to the primary antisera (TH: Millipore Ab318, mouse anti-TH, 1:4,000) to incubate overnight at 4 °C. Following primary incubation, tissue was incubated in the dark in secondary antisera against mouse IgG (Invitrogen A10037, Alexa Fluor 568 donkey anti-mouse, 1:500) for 1 hour at room temperature. Tissue was then blocked in 10% normal goat serum for 1 hour at room temperature before being incubated in the primary antisera against GFP (Abcam Ab290, rabbit anti-GFP, 1:100,000) overnight at 4 °C in the dark. Following primary incubation, tissue was incubated in secondary antisera against rabbit IgG (Life Technologies, Grand Island, NY; A21206, Alex Fluor 488 goat anti-rabbit IgG, 1:500) for 1 hour at room temperature. Sections were mounted on subbed slides and coverslipped with Vectashield Hardset Mounting Medium (Vector Laboratories). Images were taken on a Nikon 90i fluorescence microscope with a Nikon DS-Ri1 camera. Figures were produced in Photoshop 7.0. Brightness, saturation, and sharpness were adjusted only as necessary to best replicate the immunostaining as viewed directly under the microscope.

TH and GFP double label near-infrared staining

Sections were blocked in StartingBlock T20 (TBS) Blocking Buffer (Thermo Scientific, Waltham, MA) for 1 hour and subsequently transferred to the primary antisera (TH: Millipore Ab318, mouse anti-TH, 1:4,000) to incubate overnight at 4 °C. Following primary incubation, tissue was incubated in the dark in secondary antisera against mouse IgG (LI-COR 926–32212, donkey anti-mouse IRDye 800CW, 1:500) for 1 hour at room temperature. Tissue was then blocked in StartingBlock T20 (TBS) Blocking Buffer (Thermo Scientific) for 1 hour at room temperature before being incubated in the primary antisera against GFP (Abcam Ab290, rabbit anti-GFP, 1:100,000) overnight at 4 °C in the dark. Following primary incubation, tissue was incubated in secondary antisera against rabbit IgG (LI-COR 925–68021, goat anti-rabbit IRDye 680LT, 1:500) for 1 hour at room temperature. Sections were mounted on subbed slides, dehydrated via ascending ethanol washes, cleared with xylene, and coverslipped with Cytoseal. Multiplexed signal intensities were imaged with both 700 and 800 nm channels in a single scan with a resolution of 42 μm and depth set to 1.0 mm using the Odyssey infrared image system (LI-COR Biosciences, Lincoln, NE).

GFP/NeuN/glia immunofluorescence

A 1 in 12 series of sections were blocked in 10% normal donkey serum for 1 hour and subsequently transferred to the primary antisera (NeuN: Millipore Ab377, mouse anti-NeuN 1:1,000) to incubate overnight at 4 °C. Following primary incubation, tissue was incubated in the dark in secondary antisera against mouse IgG (Invitrogen A10037, Alexa Fluor 568 donkey anti-mouse, 1:500) for 1 hour at room temperature. Tissue was then blocked in 10% normal goat serum for 1 hour at room temperature before being incubated in the primary antisera against GFAP (Abcam AB7260, rabbit anti-GFAP, 1:10,000) or Iba-1 (Wako 019-19741, rabbit anti-Iba-1, 1:1,000) overnight at 4 °C in the dark. Following primary incubation, tissue was incubated in secondary antisera against rabbit IgG (LI-COR 925–68021, goat anti-rabbit IRDye 680LT, 1:500) for 1 hour at room temperature. Sections were mounted on subbed slides and coverslipped with Vectashield Hardset Mounting Medium (Vector Laboratories). Images were taken on a Nikon 90i fluorescence microscope with a Nikon DS-Ri1 camera. Figures were produced in Photoshop 7.0. Brightness, saturation, and sharpness were adjusted only as necessary to best replicate the immunostaining as viewed directly under the microscope.

RNA isolation and cDNA synthesis

RNA was isolated using the QIAshredder (Qiagen, Valencia, CA) and RNeasy Plus Mini kit (Quiagen). The Quiagen protocol for purification of total RNA from animal tissue was used. RNA from tissue was then converted into cDNA using SuperScript VILO Master Mix (Life Technologies). The RNA was assumed to be converted 100% to cDNA.

GFP qPCR

GFP qPCR reactions were carried out with 1× TaqMan Universal Mastermix (ABI, Carlsbad, CA), and a customized TaqMan gene expression assay kit for GFP (ABI). This kit includes 6,000 pmoles of the TaqMan MGB-fluorescent probe and 10,000 pmoles of each manufactured primer. Forward (R) and reverse (L) primers, as well as the probe (P) sequence were synthesized by ABI. The sequences were as follows: R: AGACCATATGAAGCAGCATGACTTTT, L: GTCTTGTAGTTCCCGTCATCTTTGA, P: 5′6FAM CTCCTGCACATAGCCC MGBNFQ. A total of 20 ng of cDNA was added to each 50 μl reaction mixture which also contained 150 nmol/l forward and 150 nmol/l reverse primers, a 150 nmol/l probe sequence, and TaqMan master mix. qPCR reactions to control for cDNA quantities were run using Glyceraldehyde 3-phosphate dehydrogenase (GAPDH) (Life Technologies 4352338E) as an endogenous control that is not altered with advanced age in F344 rats. The qPCR reactions were run on an ABI 7500 real-time thermocycler using the following setup: Step 1: Incubation at 50 °C for 2 minutes. Step 2: Incubation at 95 °C for 10 minutes. Step 3: Denaturation at 95 °C for 15 seconds followed by annealing-elongation at 60 °C for 1 minute followed by data collection. Step 3 was cycled 40 times for the qPCR run. Cycle thresholds were chosen during the linear phase of amplification using the AutoC$_t$ function. All samples were run on the same plate along with a no-template control. Analysis was first carried out using the $2^{-\Delta CT}$ method[61] and Relative Expression Software Tool (REST-XL) method.[62]

RNAscope *in situ* hybridization for GFP or CBA mRNA

Young adult and aged rats from all eight vector cohorts (rAAV2/2, rAAV2/5, rAAV2/9, and LV injected in the SNpc or striatum) were used for RNAscope for GFP mRNA. Young adult and aged rats from all striatal injection cohorts

(rAAV2/2, rAAV2/5, rAAV2/9, and LV injected in the striatum) were used for RNAscope for the viral particle CβA promoter. Twenty-μm-thick tissue sections at the level of the SNpc (nigral injections) or striatum (striatal injections) were incubated in Pretreat 1 from the RNAscope Pretreatment Kit (Advanced Cell Diagnostics, Hayward, CA; 310020) for 1 hour. Sections were washed in TBS and then mounted on Gold Seal Ultrastick slides (VWR, Randor, PA; 3039) and left at room temperature overnight. Slides were then incubated for 7 minutes in Pretreat 2 at 99 °C and left to air dry 10 minutes. After Pretreat 2, slides were dipped in water, dried, dipped in 100% ethanol, dried, and then incubated with Pretreat 3 in a hybridization oven at 40 °C for 15 minutes. Slides were dried and the VS Probe for GFP (Advanced Cell Diagnostics, Hayward, CA; 409016) or a custom VS Probe for CβA was added for a 2-hour incubation in the hybridization oven. The custom VS Probe for CβA is as follows, BLAST analyses did not reveal any reactivity with potential targets like the large chimeric intron: 5′-ctagatctgaattcggtaccctag ttattaatagtaatcaattacggggtcattagttcatagcccatatatggagttccgcgttacataactt acggtaaatggcccgcctggctgaccgcccaacgacccccgcccattgacgtcaataatgacg tatgttcccatagtaacgccaatagggactttccattgacgtcaatgggtggactatttacggtaa actgcccacttggcagtacatcaagtgtatcatatgccaagtacgccccctattgacgtcaatgac ggtaaatggcccgcctggcattatgcccagtacatgaccttatgggactttcctacttggc agtacatctacgtattagtcatcgctattaccatggtcgaggtgagccccacgttctgcttcactctccc catctcccccccctcccacccccaatttttgtatttatttatttttttaattattttgtgcagcgatggggggc gggggggggggggggggcgcgcgccaggcgggcggggcggggcgaggggcgggc ggggcgaggcggagaggtcggcggcagccaatcagagcggcgcgctccgaaagtttcctttt atggcgaggcggcggcggcggcggccctataaaaagcgaagcgcgcggcgggcgggagtc gctgcgacgctgccttcgccccgtgccccgctccgccgccgcctcgcgccgcccgccccggctct gactgaccgcgttactcccacaggtgagcgggcgggacggcccttctcctccgggctgtaattagc gcttggtttaatgacggcttgtttcttttctgtggctgcgtgaaagcct-3′. Six amplification steps with the amplification buffers (Advanced Cell Diagnostics, Hayward, CA; 320600) were then performed in alternating 30- and 15-minute incubation intervals in the hybridization oven, as per kit instructions. Tissue was developed using the supplied DAB reagent (Advanced Cell Diagnostics, Hayward, CA; 320600). CβA RNAscope tissue was then counterstained for S100B (Abcam AB52642, rabbit anti-S100B, 1:1000) or NeuN (Millipore MAB377, mouse anti-NeuN, 1:500) following the same procedures as detailed for the other immunohistochemical stains with the exception that the Vector SG reagent (Vector Laboratories) was used as the chromagen. Slides were rinsed and coverslipped with Cytoseal. Images were taken on a Nikon Eclipse 90i microscope with a QICAM camera (QImaging, Surrey, British Colombia, Canada). Figures were produced in Photoshop 7.0, with brightness, saturation, and sharpness adjusted only as needed to best replicate the mRNA labeling as viewed directly under the microscope.

Stereology

Quantification of the number of GFP immunoreactive (GFPir) cells in the midbrain (nigral injected rats), GFPir cells in the striatum (striatal injected rats), and TH immunoreactive (THir) neurons in the SNpc (nigral injected rats) was completed as previously described.[33] Briefly, stereology was performed using a Nikon Eclipse 80i microscope (Nikon), StereoInvestigator software (Microbrightfield Bioscience, Williston, VT) and Retiga 4000R camera (Qimaging, Surrey, BC Canada). Using the optical fractionator probe, THir neurons in the vector injected and control hemisphere in every sixth section of the entire SN were counted at 60× magnification. GFPir cells were counted at 60× magnification in the injected hemisphere in every sixth section of the brain where GFP staining was visible. All boundaries were drawn at 1× magnification and a 50×50 counting frame was used. A Gunderson coefficient of error <0.10 was accepted. THir data are reported as total estimates of THir neurons in each hemisphere. GFPir data are reported as percent of young estimates in the analyzed hemispheres.

Counts of GFP and TH immunoreactive cells

Tiled images at 10× magnification were taken on GFP and TH immunofluorescently stained midbrain sections containing the SNpc (average of eight sections/rat) of four rats per age per cohort injected in the SNpc with GFP-expressing viral vectors. The rats chosen represented the median GFP+ cell counts at the injection site and GFP protein in the anterograde structure. Images were taken with a Nikon 90i fluorescence microscope with a Nikon DS-Ri1 with the exposure constant between images. All GFPir cells that were in focus with a clear nucleus and appeared to be counterstained with TH were manually counted to determine the total number of GFPir/THir cells in the SNpc. Total numbers of GFPir/THir cells for rat were calculated. Data is represented as the percent of the young mean GFPir/THir cells in the SNpc.

Counts of GFP/NeuN, GFP/GFAP, and GFP/Iba-1 immunoreactive cells

Tiled images at 10× magnification were taken on the 1:12 series of GFP/NeuN/GFAP and GFP/NeuN/Iba-1 immunofluorescently stained midbrain or striatal sections of three rats per age per cohort injected in the SNpc with GFP-expressing viral vectors or injected in the striatum with GFP-expressing viral vectors, respectively. The rats chosen represented the median GFP+ cell counts at the injection site and GFP protein in the anterograde structure. Images were taken with a Nikon 90i fluorescence microscope with a Nikon DS-Ri1 with the exposure constant between images. All GFPir cells that were in focus with a clear nucleus and appeared to be counterstained with NeuN, GFAP, or Iba-1 were manually counted to determine the total number of GFPir/NeuNir, GFPir/GFAPir, and GFPir/Iba-1ir cells. Total numbers of these categories of cells were collected for each rat and then represented as the percent of GFPir cells that were NeuNir, GFAPir, or Iba-1ir.

Near-infrared signal intensity and striatal transduction area measurements

Scans were obtained of the 1:6 series of tissue stained with the LI-COR near-infrared secondary antibodies and used to determine GFP signal intensity and the area of GFP expression. For GFP signal intensity, boundaries were drawn around the entire striatum using the 800 nm channel (TH) and outlined freehand using the LI-COR Image Studio 3.1 software to obtain an average signal strength. Reported integrated intensity measurements of GFP expression were collected using the 700 nm channel and were normalized to background levels obtained in the right hemisphere striatum on the first section per brain. Data were represented as the mean striatal GFP integrated intensity measurement per brain. For GFP transduction area, boundaries were drawn directly around the area of GFP expression using the 700 nm channel (GFP) and outlined freehand using the LI-COR Image Studio 3.1 software (LI-COR Biosciences, Lincoln, NE). The individual drawing the boundaries around the transduction area was blinded to the age of the brains. The representative image was produced in Photoshop 7.0.

Comparisons between vectors

For comparisons between vector cohorts in Figures 6 and 7, Western blots were rerun to include striatal or SNpr samples on one blot to reduce variability. Due to space constraints, only the samples with median GFP protein amounts from the original western blots were run for each group. In addition, only rAAV2/5-injected rats at the 2.0×10^{12} genomes/ml were used to normalize titer between rAAV pseuodtypes for all comparisons between vectors. All data are presented as the raw numbers that were reported as percent of young in earlier figures.

Statistical analyses

All statistical tests were completed using IBM SPSS statistics software (version 22.0, IBM, Armonk, NY). Graphs were created using GraphPad Prism software (version 6, GraphPad, La Jolla, CA). To compare young adult vs. aged rats injected in the same structure with the identical vector construct independent samples t-tests were used. Results of THir SNpc neuron quantification were analyzed with two-way repeated measures analysis of variance with two treatment factors, age and hemisphere. When appropriate, Bonferroni *post hoc* analyses were used on analysis of variance tests to determine significance between individual groups. For the qPCR gene expression study, fold changes for the GFP gene were normalized to the GAPDH gene expression and calculated before being subjected to t-test analysis using the REST-XL.[62] For comparisons between vectors in Figures 6 and 7, a two-way analysis of variance was run with Bonferroni *post hoc* tests to determine significance between individual groups using the harmonic mean of the group sizes to account for unequal sample sizes.

CONFLICT OF INTEREST

ACKNOWLEDGMENTS

REFERENCES

1. O'Connor, DM and Boulis, NM (2015). Gene therapy for neurodegenerative diseases. *Trends Mol Med* **21**: 504–512.

2. Choudhury, SR, Hudry, E, Maguire, CA, Sena-Esteves, M, Breakefield, XO and Grandi, P (2016). Viral vectors for therapy of neurologic diseases. *Neuropharmacology* (epub ahead of print). DOI: 10.1016/j.neuropharm.2016.02.013.

3. Marks Jr, WJ, Bartus, RT, Siffert, J, Davis, CS, Lozano, A, Boulis, N, *et al.* (2010). Gene delivery of AAV2-neurturin for Parkinson's disease: a double-blind randomized, controlled trial. *Lancet*, **9**: 1164–1172.

4. Tuszynski, MH, Yang, JH, Barba, D, U, HS, Bakay, RA, Pay, MM *et al.* (2015). Nerve growth factor gene therapy: activation of neuronal responses in Alzheimer disease. *JAMA Neurol* **72**: 1139–1147.

5. Nobre, RJ and Almeida, LP (2011). Gene therapy for Parkinson's and Alzheimer's diseases: from the bench to clinical trials. *Curr Pharm Des* **17**: 3434–3445.

6. Combs, B, Kneynsberg, A and Kanaan, NM (2016). Gene therapy models of Alzheimer's disease and other dementias. *Methods Mol Biol* **1382**: 339–366.

7. Fischer, DL, Gombash, SE, Kemp, CJ, Manfredsson, FP, Polinski, NK, Duffy, MF *et al.* (2016). Viral vector-based modeling of neurodegenerative disorders: Parkinson's disease. *Methods Mol Biol* **1382**: 367–382.

8. Van der Perren, A, Toelen, J, Taymans, JM, and Baekelandt, V. (2012). Using recombinant adeno-associated viral vectors for gene expression in the brain. *Neuromethods* **65**: 47–68.

9. Cummings, JL, Banks, SJ, Gary, RK, Kinney, JW, Lombardo, JM, Walsh, RR *et al.* (2013). Alzheimer's disease drug development: translational neuroscience strategies. *CNS Spectr* **18**: 128–138.

10. Stocchi, F and Olanow, CW (2013). Obstacles to the development of a neuroprotective therapy for Parkinson's disease. *Mov Disord* **28**: 3–7.

11. Maguire, CA, Ramirez, SH, Merkel, SF, Sena-Esteves, M and Breakefield, XO (2014). Gene therapy for the nervous system: challenges and new strategies. *Neurotherapeutics* **11**: 817–839.

12. Emborg, ME, Moirano, J, Raschke, J, Bondarenko, V, Zufferey, R, Peng, S *et al.* (2009). Response of aged parkinsonian monkeys to *in vivo* gene transfer of GDNF. *Neurobiol Dis* **36**: 303–311.

13. Palfi, S, Gurruchaga, JM, Ralph, GS, Lepetit, H, Lavisse, S, Buttery, PC *et al.* (2014). Long-term safety and tolerability of ProSavin, a lentiviral vector-based gene therapy for Parkinson's disease: a dose escalation, open-label, phase ½ trial. *Lancet* **383**: 1138–1146.

14. Herzog, CD, Brown, L, Gammon, D, Kruegel, B, Lin, R, Wilson, A *et al.* (2009). Expression, bioactivity, and safety 1 year after adeno-associated viral vector type 2-mediated delivery of neurturin to the monkey nigrostriatal system support cere-120 for Parkinson's disease. *Neurosurgery* **64**: 602–12; discussion 612.

15. Kordower, JH, Emborg, ME, Bloch, J, Ma, SY, Chu, Y, Leventhal, L *et al.* (2000). Neurodegeneration prevented by lentiviral vector delivery of GDNF in primate models of Parkinson's disease. *Science* **290**: 767–773.

16. Bartus, RT, Herzog, CD, Chu, Y, Wilson, A, Brown, L, Siffert, J *et al.* (2011). Bioactivity of AAV2-neurturin gene therapy (CERE-120): differences between Parkinson's disease and nonhuman primate brains. *Mov Disord* **26**: 27–36.

17. Björklund, A, Kirik, D, Rosenblad, C, Georgievska, B, Lundberg, C and Mandel, RJ (2000). Towards a neuroprotective gene therapy for Parkinson's disease: use of adenovirus, AAV and lentivirus vectors for gene transfer of GDNF to the nigrostriatal system in the rat Parkinson model. *Brain Res* **886**: 82–98.

18. Marks, WJ Jr, Bartus, RT, Siffert, J, Davis, CS, Lozano, A, Boulis, N *et al.* (2010). Gene delivery of AAV2-neurturin for Parkinson's disease: a double-blind, randomised, controlled trial. *Lancet Neurol* **9**: 1164–1172.

19. Collier, TJ, Sortwell, CE and Daley, BF (1999). Diminished viability, growth, and behavioral efficacy of fetal dopamine neuron grafts in aging rats with long-term dopamine depletion: an argument for neurotrophic supplementation. *J Neurosci* **19**: 5563–5573.

20. Collier, TJ, O'Malley, J, Rademacher, DJ, Stancati, JA, Sisson, KA, Sortwell, CE *et al.* (2015). Interrogating the aged striatum: robust survival of grafted dopamine neurons in aging rats produces inferior behavioral recovery and evidence of impaired integration. *Neurobiol Dis* **77**: 191–203.

21. Nanou, A and Azzouz, M (2009). Gene therapy for neurodegenerative diseases based on lentiviral vectors. *Prog Brain Res* **175**: 187–200.

22. Reimsnider, S, Manfredsson, FP, Muzyczka, N and Mandel, RJ (2007). Time course of transgene expression after intrastriatal pseudotyped rAAV2/1, rAAV2/2, rAAV2/5, and rAAV2/8 transduction in the rat. *Mol Ther* **15**: 1504–1511.

23. Davidson, BL, Stein, CS, Heth, JA, Martins, I, Kotin, RM, Derksen, TA *et al.* (2000). Recombinant adeno-associated virus type 2, 4, and 5 vectors: transduction of variant cell types and regions in the mammalian central nervous system. *Proc Natl Acad Sci USA* **97**: 3428–3432.

24. Leone, P, Shera, D, McPhee, SW, Francis, JS, Kolodny, EH, Bilaniuk, LT, *et al.* (2012). Long-term follow-up after gene therapy for canavan disease. *Sci Transl Med* **19**: 165ra163.

25. Wu, K, Meyers, CA, Guerra, NK, King, MA and Meyer, EM (2004). The effects of rAAV2-mediated NGF gene delivery in adult and aged rats. *Mol Ther* **9**: 262–269.

26. Polinski, NK, Gombash, SE, Manfredsson, FP, Lipton, JW, Kemp, CJ, Cole-Strauss, A *et al.* (2015). Recombinant adenoassociated virus 2/5-mediated gene transfer is reduced in the aged rat midbrain. *Neurobiol Aging* **36**: 1110–1120.

27. Klein, RL, Dayton, RD, Diaczynsky, CG and Wang, DB (2010). Pronounced microgliosis and neurodegeneration in aged rats after tau gene transfer. *Neurobiol Aging* **31**: 2091–2102.

28. clinicaltrials.gov. 2015. *AAV2-GDNF for Advanced Parkinson s Disease (NCT01621581)*. www.clinicaltrials.gov/ct2/show/NCT01621581?term=gdnf&rank=1.

29. Gao, J, Miao, H, Xiao, CH, Sun, Y, Du, X, Yuan, HH *et al.* (2011). Influence of aging on the dopaminergic neurons in the substantia nigra pars compacta of rats. *Curr Aging Sci* **4**: 19–24.

30. Burger, C, Gorbatyuk, OS, Velardo, MJ, Peden, CS, Williams, P, Zolotukhin, S *et al.* (2004). Recombinant AAV viral vectors pseudotyped with viral capsids from serotypes 1, 2, and 5 display differential efficiency and cell tropism after delivery to different regions of the central nervous system. *Mol Ther* **10**: 302–317.

31. McFarland, NR, Lee, JS, Hyman, BT and McLean, PJ (2009). Comparison of transduction efficiency of recombinant AAV serotypes 1, 2, 5, and 8 in the rat nigrostriatal system. *J Neurochem* **109**: 838–845.

32. Kells, AP, Forsayeth, J and Bankiewicz, KS (2012). Glial-derived neurotrophic factor gene transfer for Parkinson's disease: anterograde distribution of AAV2 vectors in the primate brain. *Neurobiol Dis* **48**: 228–235.

33. Ciesielska, A, Mittermeyer, G, Hadaczek, P, Kells, AP, Forsayeth, J and Bankiewicz, KS (2011). Anterograde axonal transport of AAV2-GDNF in rat basal ganglia. *Mol Ther* **19**: 922–927.

34. Ryazanov, AG and Nefsky, BS (2002). Protein turnover plays a key role in aging. *Mech Ageing Dev* **123**: 207–213.

35. Grabinski, TM, Kneynsberg, A, Manfredsson, FP and Kanaan, NM (2015). A method for combining RNAscope in situ hybridization with immunohistochemistry in thick free-floating brain sections and primary neuronal cultures. *PLoS One* **10**: e0120120.

36. Yurek, DM, Hasselrot, U, Cass, WA, Sesenoglu-Laird, O, Padegimas, L and Cooper, MJ (2015). Age and lesion-induced increases of GDNF transgene expression in brain following intracerebral injections of DNA nanoparticles. *Neuroscience* **284**: 500–512.

37. Weller, ML, Stone, IM, Goss, A, Rau, T, Rova, C and Poulsen, DJ (2008). Selective overexpression of excitatory amino acid transporter 2 (EAAT2) in astrocytes enhances neuroprotection from moderate but not severe hypoxia-ischemia. *Neuroscience* **155**: 1204–1211.

38. Cannon, JR, Sew, T, Montero, L, Burton, EA and Greenamyre, JT (2011). Pseudotype-dependent lentiviral transduction of astrocytes or neurons in the rat substantia nigra. *Exp Neurol* **228**: 41–52.

39. Dodiya, HB, Bjorklund, T, Stansell, J 3rd, Mandel, RJ, Kirik, D and Kordower, JH (2010). Differential transduction following basal ganglia administration of distinct pseudotyped AAV capsid serotypes in nonhuman primates. *Mol Ther* **18**: 579–587.

40. Lippincott-Schwartz, J, Snapp, E and Kenworthy, A (2001). Studying protein dynamics in living cells. *Nat Rev Mol Cell Biol* **2**: 444–456.

41. Nonnenmacher, M and Weber, T (2012). Intracellular transport of recombinant adeno-associated virus vectors. *Gene Ther* **19**: 649–658.

42. Summerford, C and Samulski, RJ (1998). Membrane-associated heparan sulfate proteoglycan is a receptor for adeno-associated virus type 2 virions. *J Virol* **72**: 1438–1445.

43. Qiu, J, Handa, A, Kirby, M and Brown, KE (2000). The interaction of heparin sulfate and adeno-associated virus 2. *Virology* **269**: 137–147.

44. Walters, RW, Yi, SM, Keshavjee, S, Brown, KE, Welsh, MJ, Chiorini, JA *et al.* (2001). Binding of adeno-associated virus type 5 to 2,3-linked sialic acid is required for gene transfer. *J Biol Chem* **276**: 20610–20616.

45. Shen, S, Bryant, KD, Brown, SM, Randell, SH and Asokan, A (2011). Terminal N-linked galactose is the primary receptor for adeno-associated virus 9. *J Biol Chem* **286**: 13532–13540.

46. Shen, S, Bryant, KD, Sun, J, Brown, SM, Troupes, A, Pulicherla, N *et al.* (2012). Glycan binding avidity determines the systemic fate of adeno-associated virus type 9. *J Virol* **86**: 10408–10417.

47. Hwang, BY and Schaffer, DV (2013). Engineering a serum-resistant and thermostable vesicular stomatitis virus G glycoprotein for pseudotyping retroviral and lentiviral vectors. *Gene Ther* **20**: 807–815.

48. Shin, S, Tuinstra, HM, Salvay, DM and Shea, LD (2010). Phosphatidylserine immobilization of lentivirus for localized gene transfer. *Biomaterials* **31**: 4353–4359.

49. Sato, Y, Akimoto, Y, Kawakami, H, Hirano, H and Endo, T (2001). Location of sialoglycoconjugates containing the Sia(alpha)2-3Gal and Sia(alpha)2-6Gal groups in the rat hippocampus and the effect of aging on their expression. *J Histochem Cytochem* **49**: 1311–1319.

50. Sasaki, T, Akimoto, Y, Sato, Y, Kawakami, H, Hirano, H and Endo, T (2002). Distribution of sialoglycoconjugates in the rat cerebellum and its change with aging. *J Histochem Cytochem* **50**: 1179–1186.

51. Gombash, SE, Lipton, JW, Collier, TJ, Madhavan, L, Steece-Collier, K, Cole-Strauss, A *et al.* (2012). Striatal pleiotrophin overexpression provides functional and morphological neuroprotection in the 6-hydroxydopamine model. *Mol Ther* **20**: 544–554.

16

52. Ciesielska, A, Hadaczek, P, Mittermeyer, G, Zhou, S, Wright, JF, Bankiewicz, KS *et al.* (2013). Cerebral infusion of AAV9 vector-encoding non-self proteins can elicit cell-mediated immune responses. *Mol Ther* **21**: 158–166.

53. Samaranch, L, San Sebastian, W, Kells, AP, Salegio, EA, Heller, G, Bringas, JR *et al.* (2014). AAV9-mediated expression of a non-self protein in nonhuman primate central nervous system triggers widespread neuroinflammation driven by antigen-presenting cell transduction. *Mol Ther* **22**: 329–337.

54. Lowenstein, PR, Yadav, VN, Chockley, P and Castro, M (2014). There must be a way out of here: identifying a safe and efficient combination of promoter, transgene, and vector backbone for gene therapy of neurological disease. *Mol Ther* **22**: 246–247.

55. Leys, C, Ley, C, Klein, O, Bernard, P and Licata, L (2013). Detecting outliers: Do not use standard deviation around the mean, use absolute deviation around the median. *J Exp Soc Psychol* **49**: 764–766.

56. Benskey, MJ and Manfredsson, FP (2016). Lentivirus production and purification. *Methods Mol Biol* **1382**: 107–114.

57. Zolotukhin, S, Byrne, BJ, Mason, E, Zolotukhin, I, Potter, M, Chesnut, K *et al.* (1999). Recombinant adeno-associated virus purification using novel methods improves infectious titer and yield. *Gene Ther* **6**: 973–985.

58. Benskey, MJ and Manfredsson, FP (2016). Intraparenchymal stereotaxic delivery of rAAV and special considerations in vector handling. *Methods Mol Biol* **1382**: 199–215.

59. Benskey, MJ, Sandoval, IM and Manfredsson, FP (2016). Continuous collection of adeno-associated virus from producer cell medium significantly increases total viral yield. *Hum Gene Ther Methods* **27**: 32–45.

60. O'Callaghan, JP and Miller, DB (1991). The concentration of glial fibrillary acidic protein increases with age in the mouse and rat brain. *Neurobiol Aging* **12**: 171–174.

61. Schmittgen, TD and Livak, KJ (2008). Analyzing real-time PCR data by the comparative C(T) method. *Nat Protoc* **3**: 1101–1108.

62. Pfaffl, MW, Horgan, GW and Dempfle, L (2002). Relative expression software tool (REST) for group-wise comparison and statistical analysis of relative expression results in real-time PCR. *Nucleic Acids Res* **30**: e36.

Supplementary Information accompanies this paper on the *Molecular Therapy—Methods & Clinical Development* website (http://www.nature.com/mtm)